Ecological Complexity 38 (2019) 56–74

Contents lists available at ScienceDirect

Ecological Complexity

journal homepage: www.elsevier.com/locate/ecocom

Original Research Article

Accumulated marine pollution and fishery dynamics

Harald Bergland[*,a], Pål Andreas Pedersen[b], John Wyller[c]

[a] School of Business and Economics, Campus Harstad, University of Tromsø - The Arctic University of Norway, P.O. Box 1063 N-9480 Harstad Norway
[b] Nord University Business School, P.O. Box 1490, N-8049 Bodø, Norway
[c] Faculty of Science and Technology, Norwegian University of Life Sciences, P.O. Box 5003, N-1432 Ås, Norway

ARTICLE INFO

Keywords:
Pollution
Fishery dynamics
Equilibrium states

ABSTRACT

We analyze the possible impacts of pollution on a fishery by means of a dynamical systems theory approach. The proposed model presupposes that activities stimulating economic growth also cause higher emissions that remediate or accumulate in the oceans. The density of pollution is assumed to affect the fishery negatively by reducing biological growth potential and decreasing marginal willingness to pay for the fish in the market. Additionally, economic growth increases the general income and may also increase the demand for fish. We show that the modelling framework permits a unique stable equilibrium state in the regime of moderate values of the emission-remediation ratio. We also investigate how the ecological and market impacts alter both the steady state and dynamics of an open access fishery.

1. Introduction

Human activities cause a large variety of wastes that are introduced into the marine environment. Many coastal areas in the world have reported damage from pollution, with negative effects on commercial coastal and marine fisheries. See Islam and Tanaka (2004) and the references therein. Land-based emissions, including atmospheric pollutants, account for the majority of marine pollution (Williams, 1996). The main sources are human settlements, agriculture, forestry, urban development, maritime transport, tourism and other industries. In addition to taxonomy reflecting sources, pollutants are often classified by their zone of influence, defined both horizontally and vertically (e.g. local, regional or global), and also by the ability of the environment to absorb pollutants.

In economics, contaminants for which the environment has little or no absorptive capacity are often termed stock pollutants (Haavelmo, 1971; Keeler et al., 1971; Tietenberg and Lewis, 2014), since these contaminants accumulate over time as emissions enter the environment (e.g heavy metals, dioxin, PCBs). For other emissions the environment has some absorptive capacity, and therefore as long as the emission rate does not exceed this absorptive capacity, wastes do not accumulate. In Watson et al. (2016) the concept of ecosystem service of waste remediation in the marine environment is assessed. Here the waste types are divided into three main groups: (*a*) Nutrients and organic matter, (*b*) Biological wastes/contaminants and (*c*) Persistent contaminants.

A distinction between these forms of waste can be made in terms of their movement through the marine system and their potential to be broken down by abiotic and biotic processes. The more slowly a waste is cycled the greater the chance of harmful effects. For instance, normal components of natural ecosystems will likely be broken down and completely re-cycled by the system or transformed into less harmful organic matter (Watson et al., 2016). However, one of the main ocean pollutants is reactive nitrogen, mainly as runoff from agriculture production, human refuse and sewage. Nitrogen pollution may lead to coastal eutrophication, algal blooms, and oxygen depletion. In extreme cases, it could be harmful for any marine life (Perrings, 2016).

During recent decades some natural and synthetic wastes have become more prevalent in the marine environment (e.g. pesticides, fertilizers, metals and other manufactured goods) and thereby have become a serious threat to the environment due to their persistence, toxicity and ability to accumulate through the food chain - see Watson et al. (2016) and the references therein. Furthermore, in recent years extra attention has been given to plastic contamination in the marine environment (e.g. Bråte et al., 2016; Gibb et al., 2017; Hallanger and Gabrielsen, 2018).

This serves as background for the present paper. We model the possible ecological and market effects of pollution and economic growth on a fishery, using a dynamical systems theoretical approach. We consider a single species commercial fishery in a particular coastal region. The proposed dynamical model is conceptual in the sense that we explore some possible impacts on the fishery concerned. Our main focus are the economic and biological conditions in the fishery, and

* Corresponding author.
E-mail address: harald.bergland@uit.no (H. Bergland).

https://doi.org/10.1016/j.ecocom.2019.03.001
Received 9 January 2019; Received in revised form 22 February 2019; Accepted 2 March 2019

how this renewable resource harvest activity could be affected by economic growth and pollution. The first part of the model describes the development in production per capita, which measures the emissions of both production and consumption activity on the marine environment. Here we assume exogenous economic growth together with the capacity of the marine environment to self-clean. This part of the model is inspired by discussions in Haavelmo (1971) and Flaaten (2018). We assume that the flow of emissions affects the ability of the marine environment to remediate the waste substances. The second part of the model captures both the biological and the economic impacts of growth and pollution on a commercial fishery. This element of the model is an extended version of standard dynamic fishery models (e.g. Clark, 2010; Copes, 1970; Smith, 1969), and used in similar analyses by Hoagland et al. (2003), Mikkelsen (2007), Foley et al. (2012), and Perrings (2016). Beyond this application, the generalized Lotka - Volterra type systems have been extensively investigated in population dynamics, see for instance (Drossel et al., 2004; Hofbauer and Sigmund, 1998; Martinez et al., 2006; Paul et al., 2016; Smith, 1995).

The present paper is organized as follows: In Section 2 we present our modeling framework. Section 3 is devoted to the analysis of the model. Here we transform the actual system to a nondimensional form by means of scaling, before proceeding to the study of the existence and stability of equilibrium points. In Section 3 we elaborate on special aspects of the model, and present some numerical illustrations of its dynamics. Section 4 consists of concluding remarks and an outlook. Appendix A contains a generalization of the economic growth function and the self cleaning ability introduced in Section 2. Finally, important aspects of the mathematical structure of the modeling framework are explored in Appendix B, and the conditions for the existence of interior equilibrium points are explored in Appendix C.

2. Model

The model consists of two main parts or blocks. The first part describes the economic growth and the associated emission to the marine environment (Section 2.1). The second part is a modified fishery model which includes biological and economic impacts from economic growth and pollution (Section 2.2).

2.1. Economic growth and pollution

Let Y be time dependent production per capita, and assume that Y is governed by means of an economic growth equation

$$\frac{dY}{dt} = rf(Y;\bar{Y}) \tag{1}$$

where f is termed *the economic growth function*. The function f on the RHS of (1) is a smooth realvalued function on the interval $[0, \infty)$ and satisfies the following properties:

(a) For $0 \le Y < \bar{Y}$, $f(Y;\bar{Y}) > 0$ whereas for $Y > \bar{Y}$ we have $f(Y;\bar{Y}) < 0$.
(b) There is a function $\tilde{f}$ such that

$$f(Y;\bar{Y}) = C\tilde{f}\left(\frac{Y}{C};\frac{\bar{Y}}{C}\right) \quad \text{for all real } C \tag{2}$$

Here the parameters $\bar{Y}$ and C have the same dimension as Y: $[Y] = [\bar{Y}] = [C]$. The property (2) is referred to as the *homogeneity property*. Moreover, r has the dimension inverse time whereas the dimension of f is equal to the dimension of Y.[1] $\bar{Y}$ is the unique zero of f i.e.

$$f(\bar{Y};\bar{Y}) = 0 \tag{3}$$

The parameter r measures the rate of change in production per capita. By assumption, $r \ge 0$. The zero-growth case, i.e. $r = 0$, is a special case in which one considers a constant per capita income i.e. $Y(t) = Y_0$. It satisfies the saturation property.

$$\lim_{t\to\infty} Y(t) = \bar{Y} \tag{4}$$

This means that $Y = \bar{Y}$ is an asymptotically stable equilibrium point of the system (1).

When we propose Eq. (1), we have implicitly assumed that the economic development in production per capita is determined by external factors not specified in our model. Firstly, this means that the fishery under consideration only has a marginal influence on the level of economic growth, implying that it is possible to ignore this effect. Secondly, we do not explicitly discuss the factors affecting the level of economic growth, such as population growth, technical progress, investment in human capital, research and development etc. These factors could be incorporated in the modelling framework by following the line of thought elaborated in Appendix A - i.e. by assuming that the economics growth function depends on several parameters and obey a generalized homogeneity property. Our specification of economic growth means the existence of a unique long run saturation level for the production per capita given by $\bar{Y}$. This restrictive assumption is made as an analytical simplification, since we do not focus on explaining economic growth.[2] However, in our forthcoming analyses, we will see how a change in $\bar{Y}$ affects the dynamics and equilibrium states in the fishery.

We then outline the dynamical evolution for the time-dependent harmful pollution. Production and consumption activity causes emissions of harmful substances to the marine environment. Let Z denote the time dependent flow of pollution. This represents the harmful residual emissions from the economic activity, i.e. waste from both production and consumption. The pollution from industrial production can be either a function of the production volume or its use of certain inputs. We will use the often assumed simplification that this flow of pollution is proportional to the production per capita Y, i.e.

$$Z = \varrho Y \tag{5}$$

The positive proportionality constant ϱ is referred to as the *emission rate*. In addition to the waste flow denoted by Z we consider accumulation of waste over time as the main environmental problem. We study the pollution problem as a renewable natural resource problem, and assume that the environment has some absorptive capacity. An early description and discussion of the self-cleaning issue can be found in Haavelmo (1971). Within environmental and resource economics the phenomenon of accumulation of waste over time has been long studied - see, for example, early contributions by Keeler et al. (1971), Haavelmo (1971), Strøm (1971), and dArge (1971). Both (Keeler et al., 1971; Strøm, 1972) consider a model where 'the stock of pollution deteriorates naturally' as a result of alternative remediation capacities. More recently, the concept of natural recycling as an ecosystem service or a self-cleaning ability has become more common (Flaaten, 2018; Førsund and Strøm, 1980; Watson et al., 2016).

We will describe this process in the following way: For small and moderate values of the pollutant density S, the degradation rate of the pollution will increase with S. When the pollutant exceeds a certain threshold, the ability of the marine environment to carry out self cleaning will be reduced and for high pollutant concentrations, it is negligible. We summarize this self cleaning ability in a positive, two times continuously differentiable function g of S, termed the *remediation capacity*. In general, g depends on a number of biological and physical parameters. In Appendix A we describe in detail the scaling property

[1] Here and in the sequel we use the notation $[Q]$ for the dimension (measurement unit) of the variable/parameter Q.

[2] $\bar{Y}$ can be interpreted as the equilibrium state in output per worker in accordance with the Solow growth model (Solow, 1956).

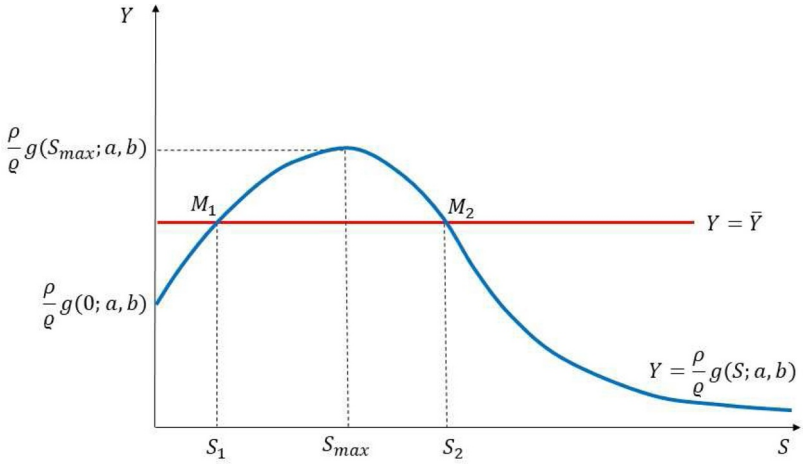

Fig. 1. The nullclines for production variable Y (red curve) and accumulated pollution S (blue curve). (For interpretation of the references to colour in this figure legend, the reader is referred to the web version of this article.)

which the remediation capacity must fulfill. For simplicity, we here consider the situation where the function g depends on only two parameters.

In line with the above description we impose the following conditions on the remediation capacity g:

(a) The function g depends on two parameters a and b which both have the same dimension as S: $[S] = [a] = [b]$
(b) $g(0; a, b) = g_0 > 0$, $\lim_{S\to\infty} g(S; a, b) = 0^{(+)}$.
(c) There is a unique positive $S = S_{\max}$ which is a global maximum point for g. This means that g is strictly increasing for $0 \le S \le S_{\max}$ and strictly decreasing for $S \ge S_{\max}$.
(d) The function g is concave (convex) for $0 \le S \le S_*$ $(S > S_*)$ where $S_* > S_{\max}$. This means that S_* is an inflection point for g.
(e) There is a function $\tilde{g}$ such that the homogeneity property

$$g(S; a, b) = C^{-1}\tilde{g}\left(\frac{S}{C}; \frac{a}{C}, \frac{b}{C}\right) \quad \text{for all real } C \tag{6}$$

is fulfilled.

We thus end up with the pollution equation

$$\frac{dS}{dt} = Z - \rho g(S; a, b) = \varrho Y - \rho g(S; a, b) \tag{7}$$

for the pollutant density S when making use of (5) and the points (a)-(e) above. The positive proportionality constant ρ is referred to as the *remediation rate*.

As comprehensively described in Watson et al. (2016) some contaminants may be broken down, re-cycled by the marine system or transformed into less harmful organic matter, whereas other contaminants accumulate over time as more emissions enter the environment (e.g heavy metals, dioxin, PCBs, plastic). Here we assume that the marine environment has some capacity of remediation or self cleaning. Fig. 1 shows a sketch of the nullclines for the production per capita Y and the accumulated pollution S.

It follows that if the nullcline for the production per capita Y satisfies the bounds

$$\frac{\rho}{\varrho}g(0; a, b) \le \bar{Y} \le \frac{\rho}{\varrho}g(S_{max}; a, b) \tag{8}$$

we have two equilibrium points of the model (1)–(7). These equilibrium points are marked with M_1 and M_2 in Fig. 1. The corresponding pollution densities are S_1 and S_2, respectively. Linear stability analysis shows that M_1 is a stable equilibrium and M_2 is unstable within the framework of (1)-(7). If $\bar{Y} > \rho g(S_{\max}; a, b)/\varrho$ we have no equilibrium point, and the pollution will steadily increase. For the case $\bar{Y} < \rho g(0; a, b)/\varrho$ it is easily seen that there is only one equilibrium point for the model (1)–(7). This point is unstable and the accumulated pollution may vanish or steadily increase[3].

2.2. The fishery

We next consider the fish harvesting sector, where the fish supply from harvesting is given by the Gordon-Schaefer production function

$$H^s = qXE \tag{9}$$

Here H^s is the time dependent supply of fish in the market (harvesting rate), X the time-dependent fish stock (biomass), E the time-dependent harvest effort and q a constant harvest efficiency rate.

We then combine the harvest function (9) with a logistic growth model for the fish population. This assumption which is often used in analyses of fisheries represents a simple way of describing the saturation of the population due to the limited food resources available. See Clark (2010) and the references therein. We assume that the fish population density X develops according to the modified logistic growth equation

$$\frac{dX}{dt} = \left[\sigma\left(1 - \frac{X + \beta S}{K}\right) - qE\right]X \tag{10}$$

Here σ is the intrinsic logistic growth rate and K the carrying capacity. The term βS in (10) thus represents a possible decrease in growth of the fish population due to the accumulated harmful pollution. Here we assume that $\beta \ge 0$. The next step consists of prescribing simplified dynamics for the effort variable E. We do this by assuming free entry and exit in proportion to profit. The expansions and the contractions of effort in the fishery sector correlate with positive and negative profits,

[3] As discussed in Perman et al. (2003) one may argue that the emission rate ϱ is not constant, but rather a linear function of the income level per capita Y. Moreover, that the flow of pollution Z is a concave function of Y. Notice that this modification will not change the qualitative features of the dynamical system modelling the interaction between the economic growth and the pollution as compared with what we obtain for the constant ϱ-case (summarized in Fig. 1): For remediation capacity g below a certain threshold, we have only one equilibrium point which is unstable. In an intermediate range for this capacity, we have two equilibrium points. The equilibrium point for which the remediation capacity g is monotonically increasing is asymptotically stable, while the equilibrium point corresponding to a monotonically decreasing remediation capacity is unstable. Finally, when the remediation capacity exceeds a certain threshold, no equilibrium points exist. For simplicity, we have not undertaken any detailed analysis of the implications of the hypothesis in Perman et al. (2003).

Table 1
The fishery-pollution model (1), (7), (10) and (16). The fundamental units are T for time (e.g. *year, month*), M for mass (e.g. *tons, kg*), E for effort (e.g. *employee, capital*) and C for currency (e.g. *Euro, Yuan* etc.).

Variables/ parameters	Biological/ economical interpretation	Measurement units (dimensions)
t	Time	T
Y	Total production value per capita	C
S	The harmful substance density (stock of pollutant)	M
X	Fish population density	M
K	Carrying capacity of the fish biomass	M
H	Production volume(harvest) in fishery	MT^{-1}
E	Effort(capital and labour) input in fishery	E
P	Market value of fish	CM^{-1}
σ	Intrinsic growth rate for the biomass	T^{-1}
β	Pollution effect on biomass growth	1
q	Fixed harvest efficiency rate	$E^{-1}T^{-1}$
r	Economy growth rate	T^{-1}
$\bar{Y}$	Long run production value per capita	C
ϱ	Emission (pollution) rate	$MC^{-1}T^{-1}$
ρ	Remediation (natural absorptive ability) rate	T^{-1}
a	Remediation capacity parameter	M
b	Remediation capacity parameter	M
a_1	Market price-volume demand impact fishery	$CM^{-2}T$
a_2	Pollution-demand impact fishery	CM^{-2}
a_3	Income-demand impact fishery	M^{-1}
$A_0 + C_0$	Potential fish price	CM^{-1}
B_0	Price-saturation constant fish supply	MT^{-1}
D_0	Price-saturation constant pollution	M
c	Cost per unit effort	$CE^{-1}T^{-1}$
λ	Speed of adjustment	EC^{-1}

and these adjustments include frictions and delays. Smith (1969) states that the entry-speed coefficients are not necessarily equal to the exit-speed coefficients. However, in order to simplify we will consider a common speed parameter λ. Similar types of enter-exit mechanisms concerning effort, which assume frictions and delays, are regularly used in fishery studies (Chakraborty et al., 2012; Ghosh and Kar, 2014; Regnier and Schubert, 2016). We take these properties into account by suggesting that the instantaneous change of rate of E is proportional to the time-dependent sector profit $\pi = PH^s - cE$, where P is the time dependent unit product price of fish and c is a constant unit price of effort i.e.

$$\frac{dE}{dt} = \lambda[PH^s - cE] \tag{11}$$

Here λ is 'speed' of adjustment in the fishery.

We assume that the demand side of the fishery market can be specified by the following time-dependent marginal willingness to pay function P:

$$P = P_1 + P_2 + a_3 Y, \quad a_3 \geq 0 \tag{12}$$

Here

$$P_1 = A_0 - a_1 B_0 \frac{H^d}{H^d + B_0}, \quad P_2 = C_0 - a_2 D_0 \frac{S}{S + D_0}$$

where

$$A_0 > 0, \quad B_0 \geq 0, \quad C_0 > 0, \quad D_0 \geq 0, \quad a_1 > 0, \quad a_2 > 0$$

Here we tacitly assume the constraints

$$a_1 B_0 \leq A_0, \quad a_2 D_0 \leq C_0 \tag{13}$$

in order to ensure that the functions P_1 and P_2 are positive for all t. These assumptions also mean that we assume P_1 to be a decreasing and convex function of the market volume H^d and to saturate on the lower positive level $A_0 - a_1 B_0$. Similar types of market-volume-mechanisms are often employed in fishery models, see e.g. Copes (1970), Smith (1969), and Flaaten and Schulz (2010). It is also assumed that P_2 decreases as a function of the harmful substance density S and saturates on the lower positive level $C_0 - a_2 D_0$. The positive constant $A_0 + C_0$ is interpreted as a potential market price for a given income per capita (Y). a_1, a_2 and a_3 are all non-negative parameters. The coefficient a_1 describes a possible standard down sloped demand mechanism, while the presence of finite a_2 suggests that there could be some negative impact on fish demand from pollution. This effect captures the possibility that the pollution may harm the quality of the fish products or affect consumers' beliefs concerning the quality of the fish and thereby reduce the willingness of consumers to pay for such products (Chen et al., 2015; Fonner and Sylvia, 2014; Garzon et al., 2016; Wessells and Anderson, 1995; Whitehead, 2006). The production per capita in the economy at time t is modelled by means of Y. Here we also interpret it as the general income level per capita. Y may have a positive influence on consumers demand for fish products, capturing the ordinary income effect on demand. Notice the interpretation of the special cases $B_0 = 0$, $D_0 = 0$ and $a_3 = 0$. $B_0 = 0$ means that the marginal willingness pay is independent of the quantity (perfect elastic demand). This special case is realistic if the fishery under consideration has only a marginal impact on the total market for relevant products. The condition $D_2 = 0$ means that the consumers are not sensitive to possible negative effects on the fish quality from pollution, or that there are no negative effects on the fish quality from pollution. Finally, $a_3 = 0$ represents the case with low or negligible income elasticity for the fish product. We also assume that the cost per unit effort c satisfies the bound

$$c < qK(A_0 + C_0) \tag{14}$$

Finally, we assume market equilibrium in the fish product market i.e.

$$H^d = H^s \tag{15}$$

for all t.

Now, by combining (9), (11), (12), and (15), we end up with the differential equation

$$\frac{dE}{dt} = \lambda\left[\left(A_0 - a_1 B_0 \frac{qXE}{qXE + B_0} + C_0 - a_2 D_0 \frac{S}{S + D_0} + a_3 Y\right)qX - c\right]E \tag{16}$$

for the effort variable E. This equation, together with the production and income Eq. (1), the population density Eq. (10) and the pollution dynamics Eq. (7) constitutes a $4D$ autonomous nonlinear dynamical system for the state variables X, E, S and Y.

The variables and the parameters in the model of differential equations are summarized in Table 1. The measurement units given in Table 1 are T for time (e.g. *year, month*), M (e.g. *tons, kg*), E for effort (e.g. *employee, capital*) and currency C (e.g. *Euro, Yuan* etc.)

3. Analysis of the model

3.1. Scaling and general properties of the model

We scale the model (1), (7), (10) and (16) by following the procedure outlined, for example, in Logan (1987). We proceed as follows: Introduce the dimensionless quantities τ, ξ, η, θ, ψ, γ_1, γ_2, γ_3, γ_4, γ_5, γ_6, γ_7, γ_8, γ_9, γ_{10}, γ_{11} and γ_{12} defined by

$$\tau = \sigma t, \quad X(t) = K\xi(\tau)$$
$$E(t) = \frac{\sigma}{q}\eta(\tau), \quad S(t) = a\theta(\tau), \quad Y(t) = \frac{\sigma a}{\varrho}\psi(\tau)$$
$$\gamma_1 = \frac{\beta a}{K}, \quad \gamma_2 = \frac{\rho}{\sigma}, \quad \gamma_3 = \frac{b}{a}, \quad \gamma_4 = \frac{r}{\sigma}$$
$$\gamma_5 = \frac{\varrho \bar{Y}}{\sigma a}, \quad \gamma_6 = \frac{\lambda q K(A_0 + C_0)}{\sigma}, \quad \gamma_7 = \frac{\lambda a_1 B_0 q K}{\sigma}, \quad \gamma_8 = \frac{B_0}{K\sigma}$$
$$\gamma_9 = \frac{\lambda a_2 D_0 q K}{\sigma}, \quad \gamma_{10} = \frac{D_0}{a}, \quad \gamma_{11} = \frac{\lambda a q K a_3}{\varrho}, \quad \gamma_{12} = \frac{\lambda c}{\sigma} \tag{17}$$

We then end up with the 4*D* autonomous dynamical system

$$\xi' = \xi F(\xi, \eta, \theta, \psi), \quad \eta' = \eta G(\xi, \eta, \theta, \psi)$$
$$\theta' = H(\xi, \eta, \theta, \psi), \quad \psi' = K(\xi, \eta, \theta, \psi) \tag{18}$$

where *F, G, H* and *K* are the functions

$$F(\xi, \eta, \theta, \psi) = 1 - \xi - \eta - \gamma_1\theta \tag{19}$$

$$G(\xi, \eta, \theta, \psi) = \gamma_6\xi - \gamma_7\frac{\xi^2\eta}{\xi\eta + \gamma_8} - \gamma_9\frac{\xi\theta}{\theta + \gamma_{10}} + \gamma_{11}\xi\psi - \gamma_{12} \tag{20}$$

$$H(\xi, \eta, \theta, \psi) = \psi - \gamma_2 R(\theta; \gamma_3) \tag{21}$$

$$K(\xi, \eta, \theta, \psi) = \gamma_4\tilde{f}(\psi; \gamma_5) \tag{22}$$

where the notation $'$ means differentiation with respect to τ. Here we have tacitly made use of the homogeneity assumptions (2) and (6) imposed on the economic growth function f and the remediation capacity g introduced in Section 2:

$$f(\psi; \gamma_5) = C^{-1}\tilde{f}(C\psi; C\gamma_5), \quad C = \frac{a\sigma}{\varrho} \tag{23}$$

$$R(\theta, \gamma_3) \equiv \tilde{g}(\theta; 1, \gamma_3) = ag(a\theta; a, b) \tag{24}$$

The function $\tilde{f}$ is referred to as the *nondimensional economic growth function*. In the subsequent numerical simulations we assume that the nondimensional economic growth function is given by

$$\tilde{f}(\psi; \gamma_5) = \gamma_5 - \psi \tag{25}$$

The function R is referred to as the *nondimensional remediation capacity*. In the subsequent numerical simulations we assume that the nondimensional remediation capacity is given by

$$R(\theta; \gamma_3) = \frac{\theta + 1}{\theta^2 + \gamma_3^2} \tag{26}$$

Due to conditions imposed on the parameters involved in our modelling framework (1), (7), (10) and (16), we notice that all the dimensionless parameters γ_1, γ_2, γ_3, γ_4, γ_5, γ_6, γ_7, γ_8, γ_9, γ_{10}, γ_{11} and γ_{12} are positive. These dimensionless parameters are listed and interpreted in Table 2. Fig. 2 summarises the model structure. Furthermore, we classify these parameters into the following three groups based on their role in the model:

- **Group 1:** Parameters in the economic growth and pollution part of the model: γ_2, γ_3, γ_4 and γ_5.
- **Group 2:** Parameters capturing impacts from the economic growth and the pollution on the fishery part of the model: γ_1, γ_9, γ_{10} and γ_{11}.
- **Group 3:** Parameters in the fishery part of the model: γ_6, γ_7, γ_8 and γ_{12}.

In the forthcoming analysis we will also make use of the two parameters ι and ω defined by

Table 2
Definition and interpretation of the nondimensional parameters γ_i ($i = 1, 2, \cdots 12$), ι and ω in the model (19)–(22).

Parameter definition	Intepretation
$\gamma_1 = \beta a/K$	The biomass growth damage rate.
$\gamma_2 = \rho/\sigma$	The relative remediation rate.
$\gamma_3 = b/a$	Remediation capacity parameter.
$\gamma_4 = r/\sigma$	The relative economic growth rate.
$\gamma_5 = \varrho\bar{Y}/\sigma a$	Relative long run emission.
$\gamma_6 = \lambda q K(A_0 + C_0)/\sigma$	Potential revenue per unit effort in fishery.
$\gamma_7 = \lambda a_1 B_0 q K/\sigma$	Harvest volume demand impact
$\gamma_8 = B_0/K\sigma$	Demand parameter market volume.
$\gamma_9 = \lambda a_2 D_0 q K/\sigma$	Pollution demand impact.
$\gamma_{10} = D_0/a$	Demand parameter pollution.
$\gamma_{11} = \lambda a q K a_3/\varrho$	Income demand impact.
$\gamma_{12} = \lambda c/\sigma$	Relative unit cost of effort in fishery.
$\iota = \gamma_5/\gamma_2$	Emission-remediation ratio.
$\omega = \gamma_{12}/\gamma_6$	Cost-potential price ratio.

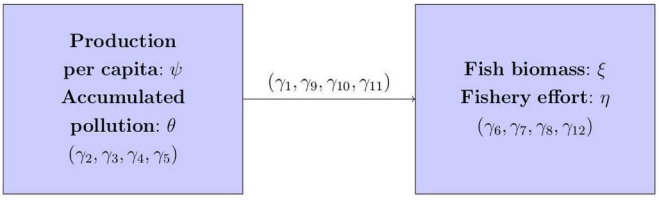

Fig. 2. Schematic representation of the pollution-fishery model (18). Nondimensional state variables (ξ, η, θ, ψ). Nondimensional parameters in the economic growth and pollution part of the model: γ_2, γ_3, γ_4 and γ_5 (Group 1), nondimensional parameters capturing impacts from the economic growth and the pollution on the fishery part of the model: γ_1, γ_9, γ_{10} and γ_{11} (Group 2), and nondimensional parameters in the fishery part of the model: γ_6, γ_7, γ_8 and γ_{12} (Group 3).

$$\iota = \frac{\gamma_5}{\gamma_2} = \frac{\varrho\bar{Y}}{\rho a}$$
$$\omega = \frac{\gamma_{12}}{\gamma_6} = \frac{c}{qK(A_0 + C_0)} \tag{27}$$

The parameters ι and ω which are listed in Table 2, are referred to as the *emission-remediation ratio* and the *cost-potential price ratio*, respectively. Notice that the condition (14) implies that $\omega < 1$.

We next describe some fundamental properties of the nondimensional system (18)–(22). Let

$$\mathbf{x} = \begin{pmatrix} \xi \\ \eta \\ \theta \\ \psi \end{pmatrix} \tag{28}$$

Introduce the vector field $\mathbf{F}$: $\mathbb{R}^4 \to \mathbb{R}^4$ defined by

$$\mathbf{F}(\mathbf{x}) = \begin{pmatrix} \xi F(\xi, \eta, \theta, \psi) \\ \eta G(\xi, \eta, \theta, \psi) \\ H(\xi, \eta, \theta, \psi) \\ K(\xi, \eta, \theta, \psi) \end{pmatrix} \tag{29}$$

Then the system (18)–(22) can conveniently be rewritten on the compact vector form

$$\frac{d\mathbf{x}}{d\tau} = \mathbf{F}(\mathbf{x}) \tag{30}$$

Since the vector field $\mathbf{F}$: $\mathbb{R}^4 \to \mathbb{R}^4$ is a smooth vectorfield, Picards theorem implies that the initial value problem of the autonomous dynamical system (30) is locally wellposed (Arnold, 1988; Guckenheimer and Holmes, 1983). Moreover, since the same vector field depends

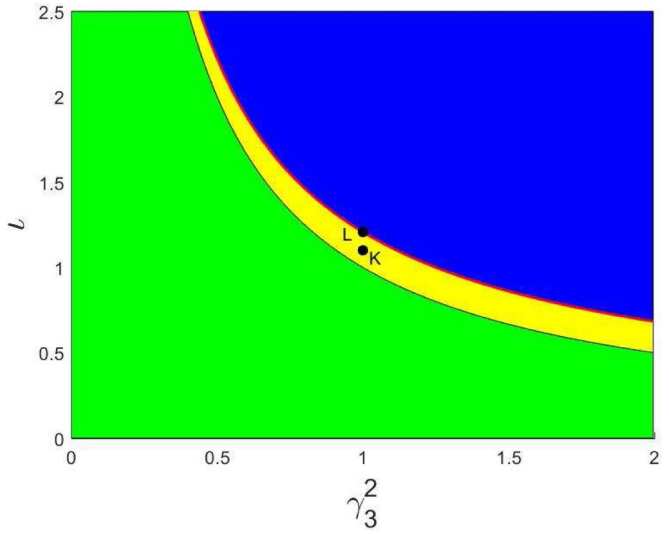

Fig. 3. The number of equilibrium points of the subsystem (32) as a function of the Group 1 - parameters γ_2, γ_3 and γ_5. The subsets $\mathcal{A}_{non}$, $\mathcal{A}_{eq,1}$, $\mathcal{A}_{eq,2}$ and C of the (γ_3^2, ι)-plane are defined by (34). Region $\mathcal{A}_{non}$ (blue shaded region) produces no equilibrium points, region $\mathcal{A}_{eq,2}$ (yellow shaded region) two equilibrium points and $\mathcal{A}_{eq,1}$ (green shaded region) one equilibrium point. The curve separating $\mathcal{A}_{eq,1}$ from $\mathcal{A}_{eq,2}$ is given by the hyperbola $\iota = \frac{1}{\gamma_3^2}$. The separatrix curve C (red curve) represents a transition between a region corresponding to two equilibrium points and a region corresponding to no equilibrium points. The point $K = (1, 1.1)$ represents the input data for the numerical computations leading to Figs. 4–5 b. The point $L = (1, \Gamma[1]) = (1, \frac{1}{2}(\sqrt{2} + 1))$ (located on the separatrix curve C) represents the input data for the numerical computations leading to Fig. 6. The separatrix curve C corresponds to a saddle-node bifurcation at the equilibrium point of the subsystem (32). Cf. the discussion of the Jacobian (36). (For interpretation of the references to colour in this figure legend, the reader is referred to the web version of this article.)

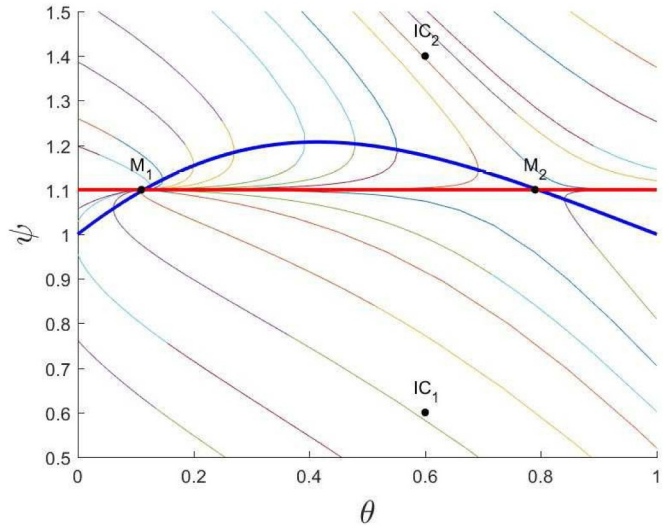

Fig. 4. Phase portrait illustrating the behavior of the pollution part (32) of the model with the nondimensional remediation capacity given by (26). The red curve is the nullcline $\psi = \gamma_5$ for the system (32) (the nondimensional production variable). The blue curve is the graph of the nondimensional accumulated pollution $\psi = \gamma_2 R(\theta; \gamma_3^2)$. The input parameters are $\gamma_2 = \gamma_3 = \gamma_4 = 1$, $\gamma_5 = 1.1$, which correspond to the point $K = (1, 1.1)$ in Fig. 3. The equilibrium point $M_1 = (\theta_e, \psi_e) = (0.11, 1.1)$ is asymptotically stable whereas the equilibrium point $M_2 = (\theta_e, \psi_e) = (0.79, 1.1)$ is a saddle point. $IC_1 = (\theta_0, \psi_0) = (0.6, 0.6)$ and $IC_2 = (\theta_0, \psi_0) = (0.6, 1.4)$ are the initial conditions for the solutions depicted in Fig. 5a and b, respectively. (For interpretation of the references to colour in this figure legend, the reader is referred to the web version of this article.)

continuously on the input parameters γ_i, $i = 1, 2, ..., 12$, any solution of the initial value problem of (30) will be continuous functions of these parameters.

In the present study we restrict ourselves to the dynamical evolution in the positive part of the phase space i.e. the region for which all the coordinates of $\mathbf{x}$ are positive. In Appendix B we prove that region Σ defined by

$$\Sigma = \{(\xi, \eta, \theta, \psi) \in \mathbb{R}^4;\ \xi > 0,\ \eta > 0,\ \theta > 0,\ \psi \geq \gamma_2 R(0; \gamma_3)\} \tag{31}$$

is an invariant region of the system (30) provided $\gamma_5 \geq \gamma_2 R(0, \gamma_3)$ (Theorem 1).

3.2. Simplified models

We first consider different parts of the model. This can provide a better understanding of how the model mechanisms work.

3.2.1. The growth and the pollution part of the model

The 2*D* subsystem

$$\theta' = \psi - \gamma_2 R(\theta; \gamma_3), \quad \psi' = \gamma_4 \tilde{f}(\psi; \gamma_5) \tag{32}$$

of the modelling framework (30) plays a crucial role in the analysis of this framework.

The problem of invariant regions of the system (32) is explored in detail in Appendix B. Here we only summarize the result of this investigation. We readily find that the set Σ_2 defined by

$$\Sigma_2 = \{(\theta, \psi) \in \mathbb{R}^2;\ \theta > 0,\ \psi > \gamma_2 R(0; \gamma_3)\} \tag{33}$$

is an invariant region of the subsystem (32) provided $\gamma_5 \geq \gamma_2 R(0; \gamma_3)$. This means that any solution of the system (32) starting in Σ_2 will remain in that region. In the complementary regime i.e. when $0 < \gamma_5 < \gamma_2 R(0; \gamma_3)$, the set Σ_2 is not an invariant region. In this case we can find solutions which will enter the region $\theta < 0$ within finite time.

Let us next examine the existence of equilibrium points and their respective stabilities. The result of this investigation is summarized in Table 3.

For the case where the nondimensional remediation capacity is modeled by means of (26) we conveniently discuss the number of equilibrium points of the subsystem (32) in the first quadrant of the θ, ψ-plane as function of the input parameters $\iota \equiv \gamma_5/\gamma_2$ and γ_3^2 in terms of a phase plot. See Table 2. The actual phase plot is depicted in Fig. 3. Here we have introduced the subsets $\mathcal{A}_{non}$, $\mathcal{A}_{eq,2}$, $\mathcal{A}_{eq,2}$ and C defined by

$$\begin{aligned} \mathcal{A}_{non} &= \{(\gamma_3^2, \iota) \in \mathbb{R}^2;\ \iota > \Gamma[\gamma_3^2]\} \\ \mathcal{A}_{eq,2} &= \{(\gamma_3^2, \iota) \in \mathbb{R}^2;\ 1/\gamma_3^2 < \iota < \Gamma[\gamma_3^2]\} \\ \mathcal{A}_{eq,1} &= \{(\gamma_3^2, \iota) \in \mathbb{R}^2;\ 0 < \iota \leq 1/\gamma_3^2\} \\ C &= \{(\gamma_3^2, \iota) \in \mathbb{R}^2;\ \iota = \Gamma[\gamma_3^2]\} \end{aligned} \tag{34}$$

Here Γ: $(0, \infty) \to (0, \infty)$ is the function defined by

$$\iota = \Gamma[\gamma_3^2] \equiv \frac{1}{2} \frac{\sqrt{1 + \gamma_3^2} + 1}{\gamma_3^2} \tag{35}$$

The curve C is derived from the nontransversal intersection condition $\iota = R(\theta; \gamma_3^2)$, $R'(\theta; \gamma_3^2) = 0$.

In Figs. 4–6 we present numerical examples which illustrate the behaviour of this part of the model corresponding to point K and L in Fig. 3.

Let us assume that we have at least one equilibrium point of the system (32). According to the results summarized in Table 3 this takes place when $0 < \iota \leq R(\theta_{\max}; \gamma_3)$. The stability problem for the equilibrium points is then easily resolved by means of the Jacobian of the system (32) evaluated at these points. The Jacobian is given by

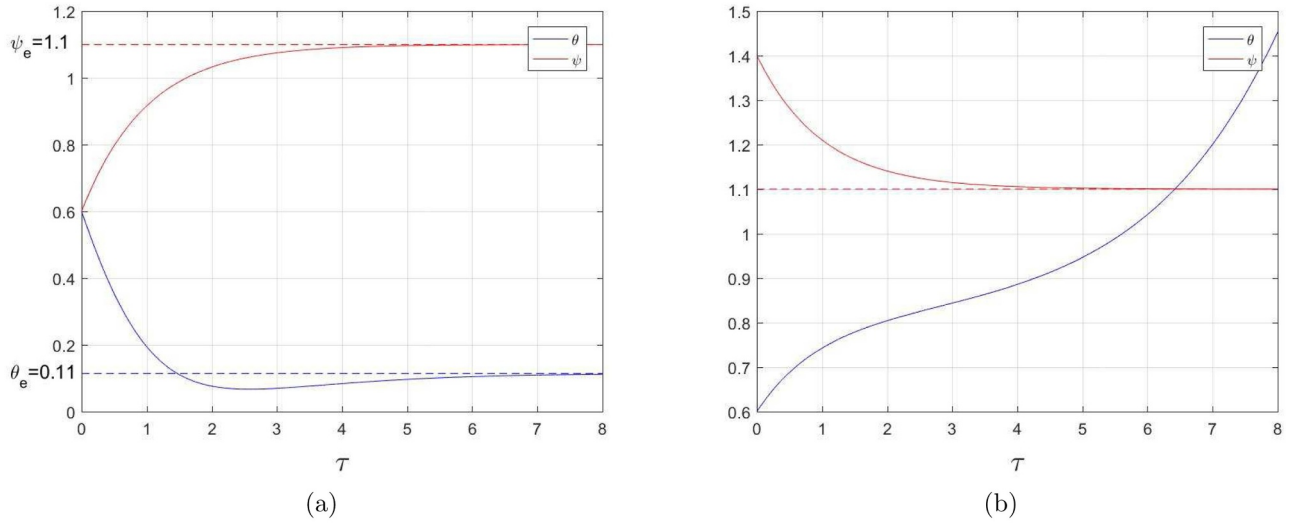

Fig. 5. Numerical example illustrating the behavior of the pollution part (32) of the model with the nondimensional remediation capacity given by (26). Input parameters as in Fig. 4. (a) The nondimensional production variable ψ (red curve) and nondimensional accumulated pollution θ (blue curve) as function of the nondimensional time τ. Initial condition: $(\theta_0, \psi_0) = (0.6, 0.6)$, i.e. point IC_1 in Fig. 4. Stable equilibrium point $M_1 = (\theta_e, \psi_e) = (0.11, 1.1)$. (b) 'Uncontrolled' pollution growth following from high initial production level. The nondimensional production variable ψ (red curve) and nondimensional accumulated pollution θ (blue curve) as function of nondimensional time τ. Initial condition: $(\theta_0, \psi_0) = (0.6, 1.4)$, i.e. point IC_2 in Fig. 4. (For interpretation of the references to colour in this figure legend, the reader is referred to the web version of this article.)

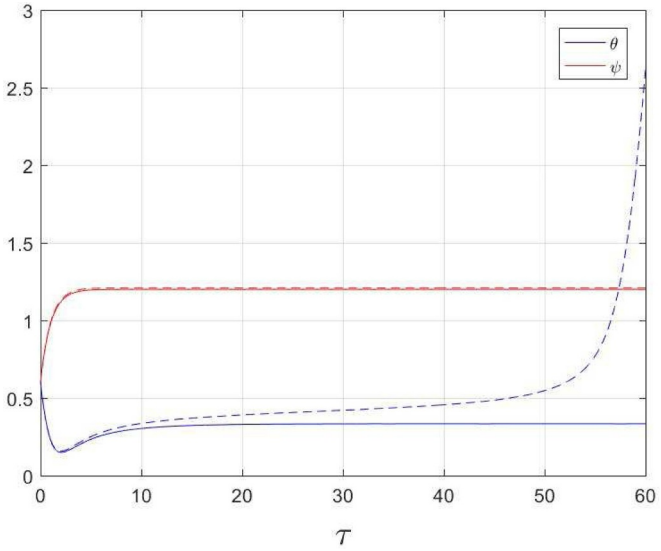

Fig. 6. Numerical example illustrating the behavior of the pollution part (32) of the model with the nondimensional remediation capacity given by (26). The nondimensional production variable ψ (red curve) and nondimensional accumulated pollution θ (blue curve) as function of the nondimensional time τ. Initial condition: $(\theta, \psi) = (0.6, 0.6)$, i.e. point IC_1 in Fig. 4. The input parameters of the bold curve are $\gamma_2 = \gamma_3 = \gamma_4 = 1$, $\gamma_5 = 1.20$ with (1,1.20) as the corresponding point in the phase plot in Fig. 3. Stable equilibrium point $(\theta_e, \psi_e) = (0.33, 1.20)$. The input parameters for the dotted curve are $\gamma_2 = \gamma_3 = \gamma_4 = 1$, $\gamma_5 = 1.21$ with (1,1.21) as corresponding point in the phase plot in Fig. 3. Notice that the points (1,1.20) and (1,1.21) belong to the subsets $\mathcal{A}_{eq,2}$ and $\mathcal{A}_{non}$, respectively, and that they are located in the vicinity of the point L in Fig. 3. We notice eventually 'uncontrolled' pollution growth following from an emission-remediation ratio above the critical level. (For interpretation of the references to colour in this figure legend, the reader is referred to the web version of this article.)

$$\mathbb{J}_2^{(l)} = \begin{pmatrix} -\gamma_2 R'(\theta_e;\, \gamma_5) & 1 \\ 0 & \gamma_4 \tilde{f}'(\gamma_5;\, \gamma_5) \end{pmatrix} \tag{36}$$

Here θ_e denotes a solution to the equation

Table 3
The number of equilibrium points of (32) as a function of the parameters $\iota \equiv \frac{\gamma_5}{\gamma_2}$ (emission-remediation ratio) and γ_3^2. $R(\theta;\, \gamma_3)$ is the nondimensional remediation capacity defined by (24) whereas $\theta_{\max}$ is defined by $S_{\max} = a\theta_{\max}$).

Parameter regime	The number of equilibrium points of (32)
$0 < \iota \le R(0;\, \gamma_3)$	1
$R(0;\, \gamma_3) < \iota < R(\theta_{\max};\, \gamma_3)$	2
$\iota = R(\theta_{\max};\, \gamma_3)$	1
$\iota > R(\theta_{\max};\, \gamma_3)$	0

$$R(\theta;\, \gamma_3) = \iota \tag{37}$$

Moreover, the notation ' means differentiation of R and $\tilde{f}$ with respect to θ and ψ, respectively. Now, due to the assumptions imposed on the function $\tilde{f}$ we have $\tilde{f}'(\psi_e;\, \gamma_3) < 0$. We thus find that $det\{\mathbb{J}_2^{(l)}\} < 0$ ($det\{\mathbb{J}_2^{(l)}\} > 0$) if and only if $R'(\theta_e;\, \gamma_5) < 0$ ($R'(\theta_e;\, \gamma_5) > 0$). Moreover, $tr\{\mathbb{J}_2^{(l)}\} < 0$, if $R'(\theta_e;\, \gamma_5) > 0$. We hence conclude that the point (θ_e, ψ_e) (with $\psi_e \equiv \gamma_5$) is a saddle point of the system (32) if $R'(\theta_e;\, \gamma_5) < 0$ whereas it is an asymptotically stable equilibrium with the framework of (32) if $R'(\theta_e;\, \gamma_5) > 0$. For $R'(\theta_e;\, \gamma_5) = 0$, we have the unique solution $\theta_e = \theta_{\max}$. In this case we have a saddle-node bifurcation at the equilibrium point $(\theta_{\max}, \psi_e)$. This situation is described by means of the separatrix curve C depicted in Fig. 3. In this case Hartman-Grobmans theorem shows that we cannot base the stability analysis of the equilibrium point on the linear analysis (Guckenheimer and Holmes, 1983). Nonlinear effects have to be taken into account in this analysis. We do not pursue this problem here.

We notice that the saddle-node bifurcation condition given by (35) can be expressed as

$$\bar{Y} = \bar{Y}_{cr} \equiv \frac{\rho a}{\varsigma}\Gamma\left[\left(\frac{b}{a}\right)^2\right]$$

when making use of (27) and the definition of γ_3. Cf. Table 2. This condition can be interpreted as the case where the flow of emission exactly equals the (maximum) remediation capacity per time unit. The previous analysis shows that when the long run production per capita level, $\bar{Y}$, exceeds the threshold value $\bar{Y}_{cr}$, there are no equilibrium points in the production and pollution part of the model. This means that we

identify as $\bar{Y}$ as a control parameter with $\bar{Y}_{cr}$ as bifurcation value.

The numerical findings are indeed consistent with the previously presented theoretical analysis. Fig. 4 displays the nullclines and the phase portrait of the subsystem (32) for a scenario with two equilibrium points. Here the two equilibrium states are marked with M_1 and M_2, consistent with the notation used in Fig. 1, and presented as point K in Fig. 3. Fig. 5a and b show the development of the nondimensional variables θ and ψ for two different scenarios. In Fig. 5a the outcome of the situation with a moderate initial production per capita is depicted (initial condition: $IC_1 = (0.6, 0.6)$). Here the solution relaxates towards the equilibrium M_1. Fig. 5b shows what can happen when the initial value of the initial production per capita is increased above a certain threshold by choosing the initial condition as $IC_2 = (0.6, 1.4)$: The accumulated pollution grows in an unbounded way as time elapses. Fig. 6 illustrates how a small perturbation in the long run production per capita causes the solution characteristics to change dramatically from a situation where the solution relaxates towards the stable equilibrium M_1 to a situation with 'uncontrolled' accumulated pollution within finite time.

3.2.2. The dynamical evolution in the case of no fish population ($\xi = 0$).

When $\xi \equiv 0$, the equation $\xi' = \xi F(\xi, \eta, \theta, \psi)$ in the hierarchy (18) is automatically fulfilled. Now by letting $\xi = 0$ in the function G defined by (20), we find that $G(\xi, \eta, \theta, \psi) = -\gamma_{12}$. Hence the equation $\eta' = \eta G(\xi, \eta, \theta, \psi)$ simplifies to the linear decay equation

$$\eta' = -\gamma_{12}\eta \tag{38}$$

in this case. The pollution part of the model is governed by the subsystem (32).

We readily observe that $\eta(\tau) \to 0$ and $\psi(\tau) \to \gamma_5$ as $\tau \to \infty$. This result is indeed what one would expect: When there are no resources available, the harvesting effort will decrease and vanish. Simple linear stability analysis reveals that the equilibrium point $(0, \theta_e, \gamma_5)$ is asymptotically stable within the framework of the dynamical system (32) and (38) when $\theta_e = \theta_-$ whereas it is a saddle point if $\theta_e = \theta_+$.

Finally, but equally important, we show in Appendix B that the subset

$$\Sigma_1 = \{(\eta, \theta, \psi) \in \mathbb{R}^3;\ \eta > 0,\ \theta > 0,\ \psi > \gamma_2 R(0; \gamma_3)\}$$

is an invariant region of the system (32) and (38) provided the constraint $\gamma_5 \geq \gamma_2 R(0; \gamma_3)$ is fulfilled i.e. a solution starting at a point in Σ_1 will remain in that region under this constraint.

3.2.3. The dynamical evolution in the case of no fishery effort ($\eta = 0$).

When $\eta \equiv 0$, the equation $\eta' = \eta G(\xi, \eta, \theta, \psi)$ is automatically fulfilled. By inserting $\eta = 0$ into the expression F defined by (19), we readily find that the equation $\xi' = \xi F(\xi, \eta, \theta, \psi)$ in the hierarchy (18) simplifies to the logistic equation

$$\xi' = (1 - \xi - \gamma_1\theta)\xi \tag{39}$$

Just as earlier, the subsystem (32) governs the pollution part of the dynamical evolution. The noncrossing property of the orbits of the system (18) implies in this case that the dynamical evolution in this case takes place in the $\eta = 0$-hyperplane. Here the stability analysis shows that the equilibrium point $(0, \theta_e, \gamma_5)$ is always unstable within the framework of (32) and (39) whereas the equilibrium point $(1 - \gamma_1\theta_e, \theta_e, \gamma_5)$ is asymptotically stable if $R'(\theta_e; \gamma_3) > 0$ and unstable if $R'(\theta_e; \gamma_3) < 0$. Here we have tacitly assumed that $0 < \theta_e < 1/\gamma_1$ in order to ensure all the coordinates of the equilibrium points are nonnegative. This result makes sense: In the case when the fish resource is not harvested, the only influence from outside is the resource growth damage from accumulated pollution. If the pollution level is stabilized at a moderate level (e.g. illustrated by point M_1 in Fig. 1) the fish stock is expected to stabilize at a certain level as well.

We also here make use of the results in Appendix B to prove that a solution starting in the subset Σ_2 defined by

$$\Sigma_2 = \{(\xi, \theta, \psi) \in \mathbb{R}^3;\ \xi > 0,\ \theta > 0,\ \psi > \gamma_2 R(0; \gamma_3)\}$$

will remain in Σ_2 provided the constraint $\gamma_5 \geq \gamma_2 R(0; \gamma_3)$ is satisfied i.e. a solution starting at a point in Σ_2 will remain in that region under this constraint.

3.3. Equilibrium points of the model

We finally examine the existence of equilibrium points in our modelling framework (30). Here we first notice that any such points must be on the form

$$(\xi, \eta, \theta, \psi) = (\xi_e, \eta_e, \theta_e, \psi_e) \tag{40}$$

if they exist. Here $\psi_e = \gamma_5$ and θ_e is a solution of (37). Notice that this equation has no solutions if $\gamma_5 > \gamma_2 R(\theta_{\max}; \gamma_3)$. This means that the system (30) has no equilibrium points when γ_5 exceeds the threshold $\gamma_2 R(\theta_{\max}; \gamma_3)$.

We conveniently divide the discussion into two subcases. In the first case we study the possibility of having equilibrium points located in the hyperplanes $\xi = 0$ and $\eta = 0$ (Section 3.3.1) whereas in the second case we search for equilibrium points for which all the coordinates are strictly positive (Section 3.3.2).

3.3.1. Equilibrium points in the hyperplanes $\xi = 0$ and $\eta = 0$

The equilibrium points of the dynamical system (30) are denoted by $(\xi_e, \eta_e, \theta_e, \psi_e)$. Here $\psi_e = \gamma_5$ whereas θ_e is the solution of (37). ξ_e and η_e satisfy $\xi_e F(\xi_e, \eta_e, \theta_e, \psi_e) = \eta_e G(\xi_e, \eta_e, \theta_e, \psi_e) = 0$. For $\xi = 0$, we will have $\eta = 0$. Hence equilibrium points in the hyperplane $\xi = 0$ are given by

$$Q_0 = (0, 0, \theta_e, \psi_e) \tag{41}$$

For the hyperplane $\eta = 0$, we readily find equilibrium points on the form

$$Q_1 = (1 - \gamma_1\theta_e, 0, \theta_e, \psi_e) \tag{42}$$

Here we tacitly assume that $\gamma_1\theta_e \leq 1$. Notice that $Q_0 = Q_1$ when $\gamma_1 = 1/\theta_e$. Notice that θ_e is either θ_- or θ_+ in the regime $R(0; \gamma_3) < \iota < R(\theta_{\max}; \gamma_3)$ (cf. Table 3). In that regime we impose the condition $\gamma_1 \leq 1/\theta_-$. In the regimes when there is only one positive solution of (37), the condition reads $\gamma_1 \leq 1/\theta_+$.

3.3.2. Equilibrium points in Σ.

We notice that the equilibrium condition $F(\xi_e, \eta_e, \theta_e, \psi_e) = 0$ (with F given by means of (19)) implies that

$$\eta_e = 1 - \gamma_1\theta_e - \xi_e, \quad \xi_e = 1 - \gamma_1\theta_e - \eta_e \tag{43}$$

Thus, in order to ensure positivity of both ξ_e and η_e, we must impose the restrictions $0 < \xi_e < 1 - \gamma_1\theta_e$, $0 < \eta_e < 1 - \gamma_1\theta_e$ and $0 < \theta_e < 1/\gamma_1$. In the sequel we will denote the interior equilibrium point by $Q_e = (\xi_e, \eta_e, \theta_e, \psi_e)$.

By plugging (43) into the equilibrium condition $G(\xi_e, \eta_e, \theta_e, \psi_e) = 0$ (with G given by means of (20)) we readily find that ξ_e satisfies the equation

$$\mathcal{P}_3(\xi_e; \alpha_0, \alpha_1, \alpha_2, \alpha_3) = 0 \tag{44}$$

where $\mathcal{P}_3$ is the cubic polynomial

$$\mathcal{P}_3(\xi_e; \alpha_0, \alpha_1, \alpha_2, \alpha_3) = \alpha_3\xi_e^3 + \alpha_2\xi_e^2 + \alpha_1\xi_e + \alpha_0 \tag{45}$$

Here the coefficients α_i, $i = 0, 1, 2, 3$ are given by

$$\alpha_3 = \gamma_7 - \gamma_6 + \gamma_9\frac{\theta_e}{\theta_e+\gamma_{10}} - \gamma_5\gamma_{11}$$

$$\alpha_2 = (\gamma_5\gamma_{11} - \gamma_7 + \gamma_6 - \gamma_9\frac{\theta_e}{\theta_e+\gamma_{10}})(1-\gamma_1\theta_e) + \gamma_{12}$$

$$\alpha_1 = (\gamma_6 - \gamma_9\frac{\theta_e}{\theta_e+\gamma_{10}} + \gamma_5\gamma_{11})\gamma_8 - \gamma_{12}(1-\gamma_1\theta_e)$$

$$\alpha_0 = -\gamma_8\gamma_{12} \tag{46}$$

This means that the equilibrium problem boils down to a study of the number of zeros of the polynomial $\mathcal{P}_3$ on the interval $(0, 1-\gamma_1\theta_e)$ as a function of the input parameters γ_i, $i = 1, 2, 3, ...,12$. In order to carry out this study we first express $\mathcal{P}_3$ in terms of the cubic polynomial Q_3 defined by

$$\mathcal{P}_3(\xi_e;\alpha_0,\alpha_1,\alpha_2,\alpha_3) = \alpha_3 Q_3(\xi_e;\mu,\nu,\gamma)$$

$$Q_3(\xi_e;\mu,\nu,\gamma) \equiv \xi_e^3 - 3\mu\xi_e^2 + 3\nu\xi_e + \gamma$$

$$\mu \equiv -\frac{\alpha_2}{3\alpha_3}, \quad \nu \equiv \frac{\alpha_1}{3\alpha_3}, \quad \gamma \equiv \frac{\alpha_0}{\alpha_3} \tag{47}$$

In Appendix C we investigate in detail the properties of the polynomial Q_3. The outcome of this analysis is that the parameters μ and γ are strictly positive whereas ν is sign-indefinite. Simple analysis reveals that Q_3 has two local extreme points for $\xi_\pm = \mu \pm \sqrt{\mu^2-\nu}$ provided $\nu < \mu^2$. Moreover, we find that $\xi_+ > 0$, $Q_3(0;\mu,\nu,\gamma) > 0$, $Q_3(\xi_-;\mu,\nu,\gamma) > 0$ and $Q_3(\xi;\mu,\nu,\gamma) \to -\infty$ as $\xi \to -\infty$. Hence Q_3 has one and only one negative real zero and maximal two positive zeros.

We proceed as follows when investigating the number of zeros as a function of the input parameters μ, ν and γ: First, we locate points for which the nontransversality condition $Q_3(\xi_+;\mu,\nu,\gamma) = Q_3'(\xi_+;\mu,\nu,\gamma) = 0$ is fulfilled. Here Q_3 is the cubic polynomial (47). By exploiting the homogeneity property

$$Q_3(\xi;\mu,\nu,\gamma) = \mu^3 Q_3(\frac{\xi}{\mu};1,\frac{\nu}{\mu^2},\frac{\gamma}{\mu^3}) \tag{48}$$

we readily find that

$$Q_3(\xi_+;\mu,\nu,\gamma) = \mu^3(\nu - \Lambda[u]) \tag{49}$$

where

$$\Lambda[u] = 2 - 3u + 2(1-u)^{3/2}, \quad u < \frac{3}{4}$$

$$\nu = \frac{\gamma}{\mu^3}, \quad u = \frac{\nu}{\mu^2} \tag{50}$$

The curve (50) separates the region in the (u, v)-parameter plane for which we have no equilibrium points of the subsystem (56) from the region where we have two equilibrium points of the same subsystem. This result is depicted in the phase plot in Fig. 7. Notice that the points in this plane are obtained through the computation procedure based on (37), (46) and (47) i.e. by

$$(\gamma_1,\cdots,\gamma_{12}) \overset{(37),(46)}{\mapsto} (\alpha_0,\alpha_1,\alpha_2,\alpha_3) \overset{(47)}{\mapsto} (\mu,\nu,\gamma) \mapsto (u,v) \tag{51}$$

Here we have introduced the subsets $\mathcal{B}_{non}$ and $\mathcal{B}_{eq}$ defined by

$$\mathcal{B}_{non} = \{(u,v) \in \mathbb{R}^2; v > \max(\Lambda[u], 0)\}$$

$$\mathcal{B}_{eq} = \left\{(u,v) \in \mathbb{R}^2; 0 < v < \Lambda[u], u < \frac{3}{4}\right\}$$

$$\mathcal{D} = \left\{(u,v) \in \mathbb{R}^2; v = \Lambda[u], u < \frac{3}{4}\right\} \tag{52}$$

The previous results regarding the number of equilibrium points of the subsystems (32) and (56) as functions of the respective input parameters together with the sign of $Q_3(\alpha_e; 1, u, v)$ (with $\alpha_e \equiv (1-\gamma_1\theta_e)\mu^{-1}$) enable us to predict the number of equilibrium points of the model (18)-(22) as a function of the input parameters γ_i, $i = 1, 2, ...,12$. The outcome of this investigation is summarized in Table 4.

Table 4
The number of equilibrium points of the system (30) in the first orthant of the phase space as a function of the input parameters γ_i, $i = 1, 2, ...,12$. The subsets $\mathcal{A}_{non}$, $\mathcal{A}_{eq,1}$, $\mathcal{A}_{eq,2}$, C, $\mathcal{B}_{non}$, $\mathcal{B}_{eq}$ and $\mathcal{D}$ are defined by means of (34) and (52). Q_3, ξ_+ and α_e are given by (47), $\xi_+ \equiv \mu + \sqrt{\mu^2-\nu}$ and $\alpha_e \equiv (1-\gamma_1\theta_e)\mu^{-1}$, respectively. ξ_+ is the local minimum point of Q_3 for the case $\nu < \mu^2$.

Parameter regime	The number of equilibrium points of (18)-(22)
$(\gamma_3^2, \iota) \in \mathcal{A}_{non}$ or $(u,v) \in \mathcal{B}_{non}$	0
$(\gamma_3^2, \iota) \in \mathcal{A}_{eq,1} \cup \mathcal{A}_{eq,2} \cup C$, $(u,v) \in \mathcal{B}_{eq} \cup \mathcal{D}$	
$\xi_+ > 1-\gamma_1\theta_e$, $Q_3(\alpha_e;1,u,v) > 0$	0
$(\gamma_3^2, \iota) \in C$, $(u,v) \in \mathcal{D}$,	
$\xi_+ < 1-\gamma_1\theta_e$	1
$(\gamma_3^2, \iota) \in C$, $(u,v) \in \mathcal{B}_{eq}$,	
$Q_3(\alpha_e;1,u,v) < 0$	1
$(\gamma_3^2, \iota) \in \mathcal{A}_{eq,1}$, $(u,v) \in \mathcal{D}$	
$\xi_+ < 1-\gamma_1\theta_e$, $Q_3(\alpha_e;1,u,v) > 0$	1
$(\gamma_3^2, \iota) \in \mathcal{A}_{eq,1}$, $(u,v) \in \mathcal{B}_{eq}$,	
$Q_3(\alpha_e;1,u,v) < 0$	1
$(\gamma_3^2, \iota) \in C$, $(u,v) \in \mathcal{B}_{eq}$	
$\xi_+ < 1-\gamma_1\theta_e$, $Q_3(\alpha_e;1,u,v) > 0$	2
$(\gamma_3^2, \iota) \in \mathcal{A}_{eq,2}$, $(u,v) \in \mathcal{D}$,	
$\xi_+ < 1-\gamma_1\theta_e$	2
$(\gamma_3^2, \iota) \in \mathcal{A}_{eq,2}$, $(u,v) \in \mathcal{B}_{eq}$,	
$Q_3(\alpha_e;1,u,v) < 0$	2
$(\gamma_3^2, \iota) \in \mathcal{A}_{eq,1}$, $(u,v) \in \mathcal{B}_{eq}$,	
$\xi_+ < 1-\gamma_1\theta_e$, $Q_3(\alpha_e;1,u,v) > 0$	2
$(\gamma_3^2, \iota) \in \mathcal{A}_{eq,2}$, $(u,v) \in \mathcal{B}_{eq}$,	
$\xi_+ < 1-\gamma_1\theta_e$, $Q_3(\alpha_e;1,u,v) > 0$	4

3.4. Stability of the equilibrium points

The Jacobian $\mathbb{J}_4$ of the vector field $\mathbf{F}$ is given by

$$\mathbb{J}_4 = \begin{pmatrix} F+\xi\frac{\partial F}{\partial\xi} & \xi\frac{\partial F}{\partial\eta} & \xi\frac{\partial F}{\partial\theta} & 0 \\ \eta\frac{\partial G}{\partial\xi} & G+\eta\frac{\partial G}{\partial\eta} & \eta\frac{\partial G}{\partial\theta} & \eta\frac{\partial G}{\partial\psi} \\ 0 & 0 & -\gamma_2 R'(\theta;\gamma_3) & 1 \\ 0 & 0 & 0 & \gamma_4\tilde{f}'(\psi;\gamma_5) \end{pmatrix} \tag{53}$$

where F and G are defined by (19) and (20), respectively. Here the notation $'$ means differentiation of the functions R and $\tilde{f}$ with respect to the respective variables θ and ψ. The structure of this Jacobian makes it possible to factorize the characteristic polynomial $\mathcal{P}_4$:

$$\mathcal{P}_4(\lambda) = det\{\lambda\mathbb{I}_4 - \mathbb{J}_4\} =$$

$$(\lambda + \gamma_4\tilde{f}'(\psi;\gamma_5))(\lambda + \gamma_2 R'(\theta))(\lambda-\lambda_+)(\lambda-\lambda_-)$$

Here

$$\lambda_\pm = \frac{1}{2}\left(tr\{\mathbb{J}_2^{(u)}\} \pm \sqrt{(tr\{\mathbb{J}_2^{(u)}\})^2 - 4det\{\mathbb{J}_2^{(u)}\}}\right) \tag{54}$$

where $\mathbb{J}_2^{(u)}$ is 2×2 - block matrix

$$\mathbb{J}_2^{(u)} = \begin{pmatrix} F+\xi\frac{\partial F}{\partial\xi} & \xi\frac{\partial F}{\partial\eta} \\ \eta\frac{\partial G}{\partial\xi} & G+\eta\frac{\partial G}{\partial\eta} \end{pmatrix} \tag{55}$$

of $\mathbb{J}_4$. Notice that $\mathbb{J}_2^{(u)}$ is the Jacobian of the $2D$ subsystem

$$\xi' = \xi F(\xi,\eta,\theta,\psi), \quad \eta' = \eta G(\xi,\eta,\theta,\psi) \tag{56}$$

Notice that the lower 2×2 - block matrix of (53) is the Jacobian of the subsystem (32).

We first investigate the stability of the boundary equilibrium points Q_0 and Q_1 given by (41) and (42), respectively. For Q_0 we find that

$$det\{\mathbb{J}_2^{(u)}\} = -\gamma_{12}(1 - \gamma_1\theta_e) < 0$$

from which it follows that Q_0 always is a saddle point. For Q_1 we have the following results: For the case $R'(\theta_e; \gamma_3) < 0$, we will have a saddle point at Q_1. In the complementary regime, it is necessary to study the invariants of the upper 2×2-block matrix $\mathbb{J}_2^{(u)}$ in order to assess the stability property. We readily find the expressions

$$det\{\mathbb{J}_2^{(u)}\} = \xi_e[\gamma_{12} + (\alpha_3 - \gamma_7)\xi_e]$$

$$tr\{\mathbb{J}_2^{(u)}\} = -\xi_e^{-1}[\xi_e^2 + det\{\mathbb{J}_2^{(u)}\}]$$

for the invariants of the matrix $\mathbb{J}_2^{(u)}$ in this case. Here α_3 is given by (46). This means that Q_1 is a saddle point if

$$\gamma_{12} < (\gamma_7 - \alpha_3)\xi_e$$

In the complementary regime

$$\gamma_{12} > (\gamma_7 - \alpha_3)\xi_e \tag{57}$$

we observe that $det\{\mathbb{J}_2^{(u)}\} > 0$, $tr\{\mathbb{J}_2^{(u)}\} < 0$. Hence, if $\theta_e = \theta_-$, the equilibrium point Q_1 will be asymptotically stable when the condition (57) is fulfilled.

The boundary equilibrium point Q_1 represents a state with no fishery effort. The interpretation of the stability condition (57) is related to the profitability of the fishery. The condition (57) is fulfilled when values of Group 2 and Group 3 parameters in combination with the level of accumulated pollution (θ_e) altogether result in an unprofitable state for the fishery. For instance, we notice that high value of the cost-potential price ratio (ι) contributes to low profitability. A strong demand pollution effect also causes a low profiatbility. The consumers willingness to pay for the fish is influenced by the accumulated marine pollution. If this sensibility is strong (represented by the value of γ_9), and/or the accumulated pollution density (θ_e) is relatively high, then a low market price has the possibility of making the fishery unprofitable. This may result in a stable equilibrium state characterized by a positive fish stock but no fishery effort.

Finally let us examine the stability of equilibrium points $(\xi_e, \eta_e, \theta_e, \psi_e)$ in the positive part of the phase space. This means that we assume $F(\xi_e, \eta_e, \theta_e, \psi_e) = G(\xi_e, \eta_e, \theta_e, \psi_e) = 0$. In this case we find that the invariants of $\mathbb{J}_2^{(u)}$, evaluated at the equilibrium point $(\xi_e, \eta_e, \theta_e, \psi_e)$ are given as

$$det\{\mathbb{J}_2^{(u)}\} = \frac{\xi_e\eta_e}{\xi_e\eta_e + \gamma_8}\mathcal{P}'_3(\xi_e; \alpha_0, \alpha_1, \alpha_2, \alpha_3) = \frac{\xi_e\eta_e\alpha_3}{\xi_e\eta_e + \gamma_8}\mu^2 Q'_3(\frac{\xi_e}{\mu}; 1, u, v)$$

$$tr\{\mathbb{J}_2^{(u)}\} = -\left(\xi_e + \gamma_7\gamma_8\frac{\eta_e\xi_e^2}{(\xi_e\eta_e + \gamma_8)^3}\right) < 0 \tag{58}$$

where $\mathcal{P}_3$ and Q_3 are the polynomials defined by (45) and (47), respectively. Here Q'_3 means differentiation of Q_3 with respect to ξ, i.e. $Q'_3(\xi; \mu, \nu, \gamma) = \frac{d}{d\xi}Q_3(\xi; \mu, \nu, \gamma)$. In the process of deriving (58) we have also exploited the homogeneity property (48).

We first consider the case when the equilibrium points are hyperbolic points i.e. the case when $R'(\theta_e; \gamma_3) \neq 0$ and $Q'_3(\xi_e; \mu, \nu, \gamma) \neq 0$. Since $\alpha_3 < 0$, we arrive at the following conclusion: If either $Q'_3(\xi_e; \mu, \nu, \gamma) > 0$ or $R'(\theta_e; \gamma_3) < 0$, the equilibrium point $(\xi_e, \eta_e, \theta_e, \psi_e)$ is a saddle point. If $Q'_3(\xi_e; \mu, \nu, \gamma) < 0$ and $R'(\theta_e; \gamma_3) > 0$, the corresponding equilibrium point is $(\xi_e, \eta_e, \theta_e, \psi_e)$ is asymptotically stable. Thus the monotonicity properties of the self cleaning function R and the equilibrium polynomial Q_3 play crucial roles in the linear stability analysis. In accordance with Hartman-Grobmans theorem we can assess the stability of the equilibrium points in this case by means of the analysis of the linearized problem. See Guckenheimer and Holmes (1983) for details.

Next, let us examine the case when the equilibrium points are nonhyperbolic. This happens when either $R'(\theta_e; \gamma_3) = 0$ or $Q'_3(\xi_e; \mu, \nu, \gamma) = 0$. Hartman-Grobmans theorem shows that the linearization procedure is inconclusive with respect to the stability assessment in this case. Nonlinear effects have to be taken into account in order to determine the stability properties. First let us consider the situation $R'(\theta_e; \gamma_3) = 0$. As pointed out in Section 3.2.1, we have saddle-node bifurcation within the framework of the $2D$ subsystem (32) in this case. For the corresponding interior equilibrium point Q_e, Shoshitaishvilis theorem implies that this equilibrium point is unstable if $Q'_3(\xi_e; \mu, \nu, \gamma) > 0$. See for example Chapter 6 in Arnold (1988). For the complementary regime i.e. when $Q'_3(\xi_e; \mu, \nu, \gamma) \leq 0$, one has to carry out a detailed analysis of the nonlinear effects to conclude about the stability. We do not pursue any details of this analysis here, however. Secondly, let us study the case when $Q'_3(\xi_e; \mu, \nu, \gamma) = 0$ and $R'(\theta_e; \gamma_3) \neq 0$. This case also represents a saddle node bifurcation with the generation/vanishing of two equilibrium points as a possible outcome. Again, by appealing to Shoshitaishvilis theorem we conclude that we have an instability if $R'(\theta_e; \gamma_3) < 0$. The complementary regime $R'(\theta_e; \gamma_3) > 0$ requires a more thorough analysis of the nonlinear effects in order to resolve the stability issue. We will not enter into a discussion of this issue here, however.

We can now exploit the results summarized in Table 4 in the stability assessment of the equilibrium states. We first notice that the separatrix curves $\mathcal{C}$ and $\mathcal{D}$ defined by means of (34) and (52) produce nonhyperbolic equilibrium points of the saddle-node type. Secondly, by appealing to Table 4 and monotonicity properties of the self cleaning function R and the equilibrium polynomial Q_3, we conclude that we have a unique asymptotically stable equilibrium point in the first orthant of the phase space in the following two parameter regimes:

1. $(\gamma_3^2, \iota) \in \mathcal{A}_{eq,2}$, $(u, v) \in \mathcal{B}_{eq}$, $Q_3(\alpha_e; 1, u, v) < 0$.
2. $(\gamma_3^2, \iota) \in \mathcal{A}_{eq,2}$, $(u, v) \in \mathcal{B}_{eq}$, $\xi_+ < 1 - \gamma_1\theta_e$, $Q_3(\alpha_e; 1, u, v) > 0$.

The subset $\mathcal{B}_{non}$ (blue shaded region in Fig. 7) gives no equilibrium points of the complete model. This represents cases where the price and cost conditions altogether make the fishery unprofitable. The subset $\mathcal{B}_{eq}$ (green shaded region Fig. 7) can give rise to a possible stable equilibrium of the complete model. This represents profitable fishing conditions.

The discussion in Section 3.2.1 shows that it is easy to identify a relevant bifurcation parameter (e.g. $\bar{Y}_{cr}$), when we consider the production and pollution part of the model isolated. However, when it comes to the bioeconomic part (56) of the model, we have the following situation: With a given set of Group 1 - parameters, all parameters belonging to Group 2 and Group 3 will influence the fishery profit. The parametric complexity of the problem makes it not particular meaningful to single out one specific bioeconomic bifurcation parameter in the subsystem (56) of the model, corresponding to points located on the red separatrix curve in Fig. 7.

3.5. Special cases of the model and numerical examples

We now consider some special cases of our model with particular emphasis on possible equilibrium states and their respective stabilities. By excluding some mechanisms and combinations of mechanisms, we separate different elements in the model. This will provide for a better understanding of how the model works. Moreover, it facilitates easier interpretations of the results. Some of these results are reported in earlier works. We will use input parameters which produce points located in the blue shaded regions of Fig. 7 in the numerical simulations.

3.5.1. No pollution and economic growth impacts ($\beta = D_0 = a_3 = 0$)

Considering the fishery part of the model, we start out by assuming no impacts from the growth and pollution part of the model. This means to assume that $\beta = D_0 = a_3 = 0$ in our modelling framework. In the dimensionless setting this assumption corresponds to $\gamma_1 = \gamma_9 = \gamma_{10} = \gamma_{11} = 0$. From (19) and (20) it follows that the non-dimensional fishery part of the model simplifies to the 2*D* system

$$\xi' = (1 - \xi - \eta)\xi \tag{59}$$

$$\eta' = \left(\gamma_6\xi - \gamma_7\frac{\xi^2\eta}{\xi\eta + \gamma_8} - \gamma_{12}\right)\eta \tag{60}$$

For the purpose of detecting equilibrium points, we conveniently express the equilibrium polynomial (45) as

$$\mathcal{P}_3(\xi_e; \alpha_0, \alpha_1, \alpha_2, \alpha_3) = \alpha_3\mathcal{R}_3(\xi_e; \mu_1, \nu_1, \iota) \tag{61}$$

where

$$\mathcal{R}_3(\xi_e; \mu_1, \nu_1, \iota) \equiv \xi_e^3 - (1 + \mu_1)\xi_e^2 + (\mu_1 - \nu_1)\xi_e + \nu_1\omega = 0 \tag{62}$$

Here

$$\mu_1 \equiv \frac{\gamma_{12}}{\gamma_6 - \gamma_7}, \quad \nu_1 \equiv \frac{\gamma_6\gamma_8}{\gamma_6 - \gamma_7}, \quad \omega \equiv \frac{\gamma_{12}}{\gamma_6}$$

We notice that the condition (13) and the definition (17) imply that $\gamma_6 > \gamma_7$. Hence $\mu_1 > 0$ and $\nu_1 > 0$. Moreover, in accordance with Table 2 and (14), we have $0 < \omega < 1$. A detailed study then reveals that the polynomial $\mathcal{R}_3$ has one and only one zero in the interval (0,1). Moreover, for this zero (denoted by ξ_e) we must have $\mathcal{R}_3'(\xi_e; \mu_1, \nu_1, \omega)) < 0$. Since $\alpha_3 < 0$, we conclude by using (58) and (61) that the equilibrium point $(\xi_e, 1 - \xi_e)$ is asymptotically stable within the framework (59) and (60). Given the fact that any solution that starts in the first quadrant remains in this quadrant, the actual equilibrium point acts as an attractor for all points in the first quadrant. Notice that the system (59) and (60) is similar to the models discussed in Smith (1969) and Copes (1970).

Now, by making the additional assumption $B_0 = 0$ (corresponding to a constant fish price), it follows that $\gamma_7 = \gamma_8 = 0$ and hence the framework (59) and (60) becomes the standard Gordon-Schaefer model

$$\xi' = (1 - \xi - \eta)\xi \tag{63}$$

$$\eta' = (\gamma_6\xi - \gamma_{12})\eta \tag{64}$$

The properties of (63) and (64) are indeed the same as those observed for (59) and (60): It has an asymptotically stable interior equilibrium point, $(\xi_e, \eta_e) = (\omega, 1 - \omega)$. Moreover, any solution of (63) and (64) in the first quadrant remains in this quadrant.

To explore how the model works, we present some numerical examples. In Table 5 we have listed the input parameters $\gamma_1, \cdots, \gamma_{12}$ of each of the examples we will consider, together with the corresponding *u, v*-coordinates of the points in the phase plot depicted in Fig. 7. Table 5 contains the input parameters for the numerical computations underlying Fig. 8a–Fig. 9b, the separate mechanism by means of the group 2 parameters (γ_1, γ_9, γ_{10}, γ_{11}) and the sensitivity analyses presented in Fig. 10a–Fig. 12b. The fourth column in Table 5 contains the stable equilibrium values for the nondimensional biomass variable ξ and the nondimensional effort variable η.

Baseline parameters belonging to the fishery part of the model are given in Table 6. By inserting these fundamental parameter values into (17) we find that $\gamma_6 = 2$, $\gamma_{12} = 1$ and $\omega = \gamma_{12}/\gamma_6 = 0.5$.

Fig. 8a and b illustrate the behaviour of the fishery part of the model for the case with a constant fish price, i.e. the system (63) and (64). A notable feature here is standard fishery adjustments under open access where the nondimensional biomass and effort variables oscillate and relaxate towards a level determined by the cost-potential price ratio

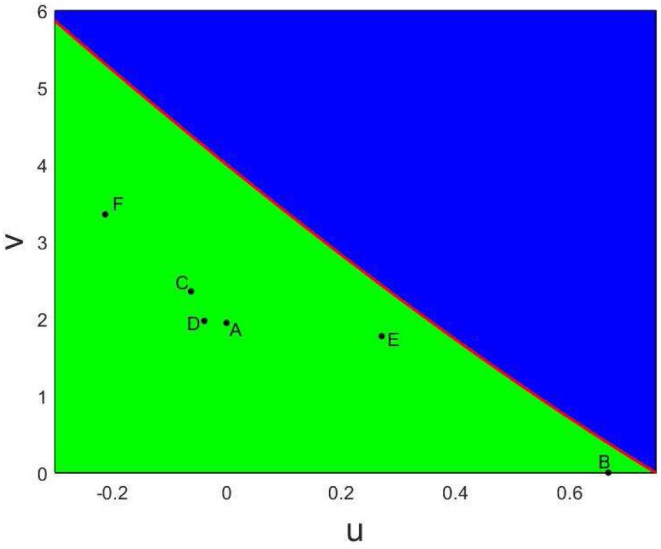

Fig. 7. The number of equilibrium points of the subsystem (56) as a function of $(u, v) = (\nu/\mu^2, \gamma/\mu^3)$ where μ, ν and γ are defined by means of (47). The subsets $\mathcal{B}_{non}$, $\mathcal{B}_{eq}$ and $\mathcal{D}$ of the (u, v)-plane are defined by means of (52). The subset $\mathcal{B}_{non}$ (blue shaded region) gives no equilibrium points of (56), whereas the subset $\mathcal{B}_{eq}$ (green shaded region) produces two equilibrium points of (56). The separatrix curve $\mathcal{D}$ (red curve) which represents the transition between $\mathcal{B}_{non}$ and $\mathcal{B}_{eq}$ gives a saddle-node bifurcation of the equilibrium points of the subsystem (56). Cf. the outcome of the stability analysis in the Section 3.4. The points *A, B, C, D, E* and *F* which are obtained by means of the computational procedure (51), are listed in Table 5 together with the corresponding input parameters $\gamma_1, \cdots, \gamma_{12}$. (For interpretation of the references to colour in this figure legend, the reader is referred to the web version of this article.)

$\omega = \gamma_{12}/\gamma_6 = c/qK(A_0 + C_0)$.[4] When the harvest volume demand impact is included, i.e. when $\gamma_7 > 0$, $\gamma_8 > 0$, as in Fig. 9a and b, we notice the same type of oscillatory development. However, since the harvest volume influences prices and makes a high catch volume less profitable, the equilibrium effort becomes lower and the biomass density higher compared to what one obtains in the constant price case.

3.5.2. Different mechanisms influencing the fishery

In order to study how changes in the level of economic growth and pollution may influence the fishery, it is convenient to consider the case with $B_0 = 0$. This means that the marginal willingness to pay is independent of the harvest volume i.e. the situation with perfect elastic demand. This parameter regime captures the situation when the fishery has a marginal impact on the total market for relevant products. By this assumption it follows that $\gamma_7 = \gamma_8 = 0$, and from (19) and (20) it follows that the nondimensional fishery part of model simplifies to

$$\xi' = (1 - \xi - \eta - \gamma_1\theta)\xi \tag{65}$$

$$\eta' = \left(\gamma_6\xi - \gamma_9\frac{\xi\theta}{\theta + \gamma_{10}} + \gamma_{11}\xi\psi - \gamma_{12}\right)\eta \tag{66}$$

In this case the equilibrium polynomial $\mathcal{P}_3$ defined by (45) can be written as

$$\mathcal{P}_3(\xi_e; \alpha_0, \alpha_1, \alpha_2, \alpha_3) = \alpha_3\xi_e Q_2(\xi_e; \mu_2, \nu_2)$$

$$Q_2(\xi_e; \mu_2, \nu_2) = \xi_e^2 + (\mu_2 - \nu_2)\xi_e - \nu_2\mu_2$$

[4] The equilibrium point $(\xi_e = \omega, \eta_e = 1 - \omega)$ corresponds to $X_e = K\xi_e = c/q(A_0 + C_0)$ and $E_e = \frac{\sigma}{q}\eta = \frac{\sigma}{q}[1 - c/q(A_0 + C_0)]$ when restoring to the dimensional quantities by means of (17). In some textbooks this equilibrium are often labeled (X_∞, E_∞). See for example Flaaten (2018).

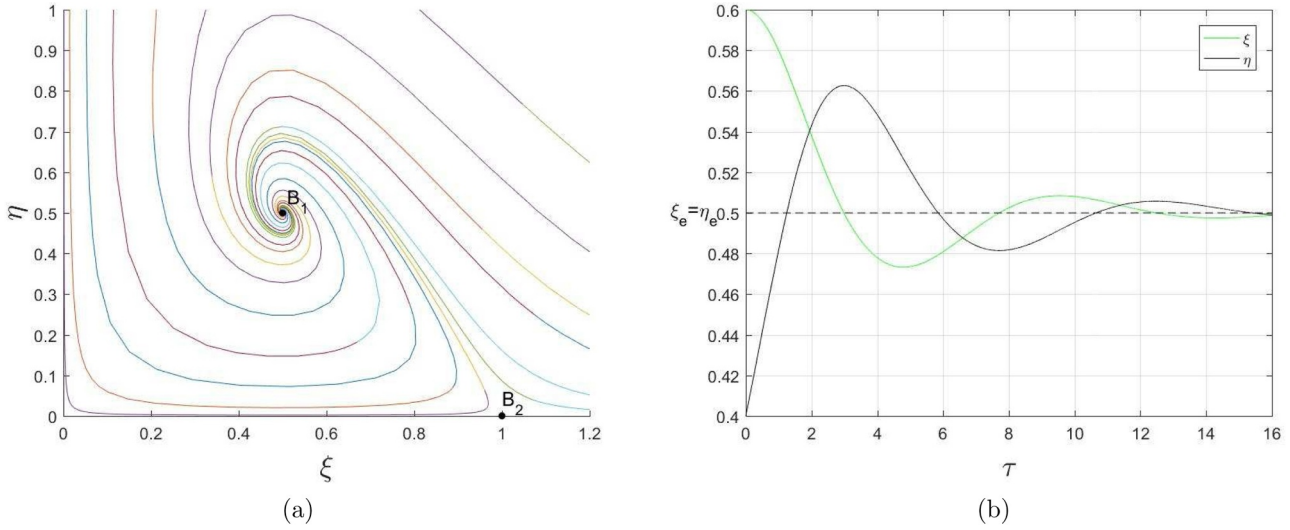

Fig. 8. Numerical example illustrating the solutions of the fishery part of the model (the system (63) and (64)). Input parameters: $\gamma_6 = 2$, $\gamma_{12} = 1$, ($\gamma_7 = \gamma_8 = 0$). This example corresponds to the point B in Fig. 7. (a) Phase portrait of the system (63) and (64). Stable equilibrium point, $B_1 = (0.5, 0.5)$. Saddle point, $B_2 = (1, 0)$. (b) The nondimensional biomass variable ξ (green curve) and nondimensional effort variable η (black curve) as a function of the nondimensional time τ. Initial condition: $(\xi_0, \eta_0) = (0.6, 0.4)$. (For interpretation of the references to colour in this figure legend, the reader is referred to the web version of this article.)

Here

$$\alpha_3 = -\gamma_6 + \gamma_9 \frac{\theta_e}{\theta_e + \gamma_{10}} - \gamma_5\gamma_{11}$$

$$\mu_2 = \frac{\gamma_{12}}{\alpha_3}, \quad \nu_2 = 1 - \gamma_1\theta_e$$

Since $\alpha_3 < 0$ it follows that $\mu_2 < 0$ whereas $0 < \nu_2 < 1$ (due to the requirement $0 < 1 - \gamma_1\theta_e < 1$). The zeros of Q_2 are given as $\xi_e^{(+)} = \nu_2$ and $\xi_e^{-} = -\mu_2$. Since $\alpha_3 < 0$, we find that $0 < \xi_e^{(-)} < \xi_e^{(+)} < 1$.

For the sake of the stability examination, we first observe that

$$\mathcal{P}_3'(\xi_e^{(\pm)}) = \alpha_3\xi_e^{(\pm)}Q_2'(\xi_e^{(\pm)})$$

Simple analysis of the quadratic polynomial Q_2 and the general stability result developed in Section 3.4 (i.e. the expressions (58) for the trace and determinant of the Jacobian $\mathbb{J}_2^{(u)}$) reveal that the interior equilibrium point $(\nu_2, 1 - \nu_2 - \gamma_1\theta_e)$ is unstable whereas the equilibrium point $(-\mu_2, 1 + \mu_2 - \gamma_1\theta_e)$ is asymptotically stable.

These results can indeed be used to assess the stability of the interior equilibrium points of the full model (30) when $\gamma_7 = \gamma_8 = 0$: Let $\theta_e = \theta_-$ be the solution to (37) for which $R'(\theta_e; \gamma_5) > 0$. The interior equilibrium point $(\nu_2, 1 - \nu_2 - \gamma_1\theta_-, \theta_-, \gamma_5)$ is unstable within the framework of the model (30) whereas the other interior equilibrium point $(-\mu_2, 1 + \mu_2 - \gamma_1\theta_-, \theta_-, \gamma_5)$ is asymptotically stable.

Furthermore, we utilize the numerical example depicted in Fig. 8a and b, to clarify the different mechanisms of economic growth and pollution on the fishery and examine the role of the Group 2 parameters i.e. γ_1, γ_9, γ_{10} and γ_{11}. These parameters both influence the stable equilibrium states and the dynamical evolution in the fishery. Table 5 summarizes how the separate mechanisms alter the coordinates of the stable equilibrium in this case.

From the third row in Table 5 we infer that when only the biomass growth impact from pollution (represented by a finite γ_1) is present, the fish stock equilibrium value remains unchanged. The explanation for

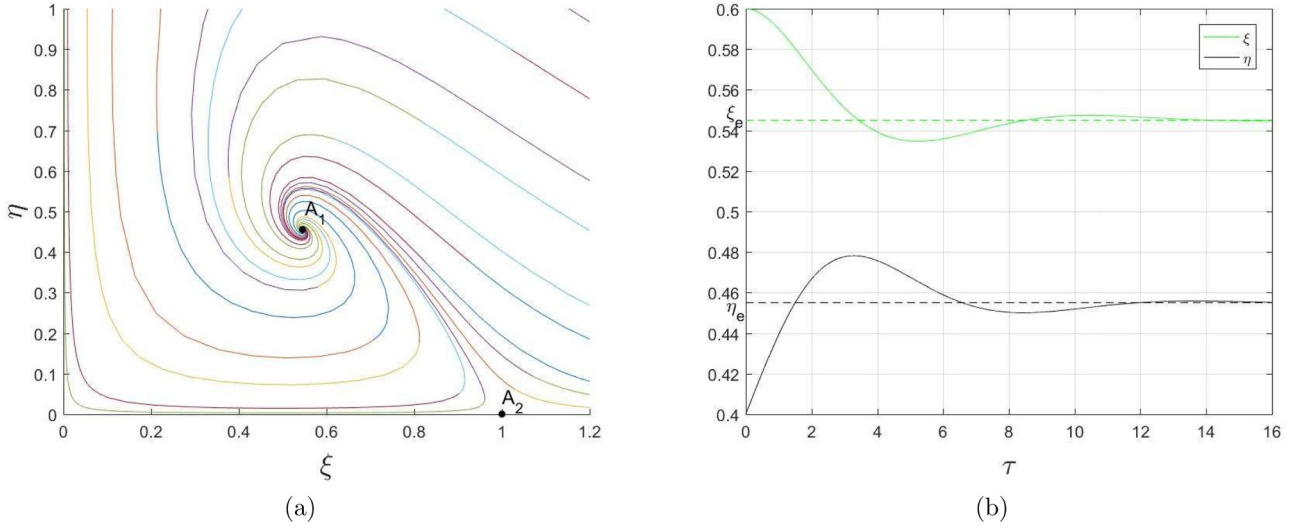

Fig. 9. Numerical example illustrating the solutions of the fishery part of the model (the system (59) and (60)). Input parameters: $\gamma_6 = 2$, $\gamma_{12} = 1$, $\gamma_7 = \gamma_8 = 1/2$. This case corresponds to point A in Fig. 7. (a) Phase portrait of the system (59) and (60). Stable equilibrium point, $A_1 = (0.545, 0.455)$. Saddle point, $A_2 = (1, 0)$. (b) The nondimensional biomass variable ξ (green curve) and nondimensional effort variable η (black curve) as a function of the nondimensional time τ. Initial condition: $(\xi_0, \eta_0) = (0.6, 0.4)$. (For interpretation of the references to colour in this figure legend, the reader is referred to the web version of this article.)

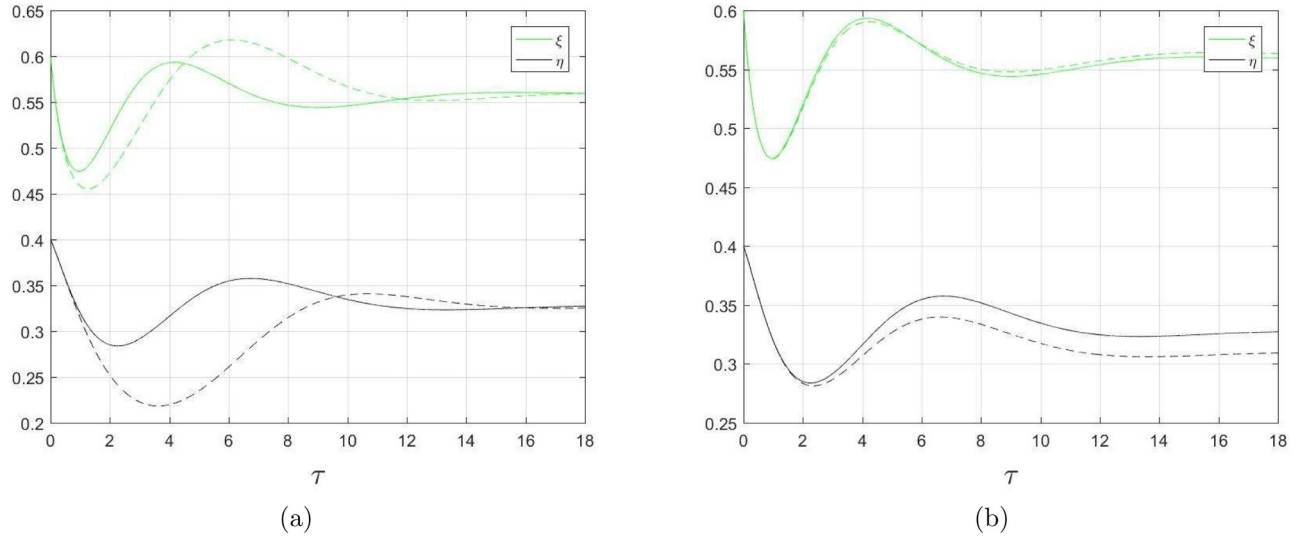

Fig. 10. Impact of 'short run' economic growth and long run level of production per capita. (a) The impact of economic growth measured by means of the nondimensional parameter γ_4. Initial condition as in Fig. 5a and Fig. 8b. The nondimensional biomass ξ (green curve) and the nondimensional effort η (black curve) as function of the nondimensional time τ (with an increased short run growth). Bold curve: The reference values given in Table 5 ($\gamma_4 = 1$) and represented in Fig. 7 as point C. Dotted curve: The reference values given in Table 5 but, $\gamma_4 = 2$. (b) The impact of long run level of production per capita. The nondimensional biomass ξ (green curve) and the nondimensional effort η (black curve) as function of the nondimensional time τ with increased long run production level measured by means of the nondimensional parameter γ_5. Bold curve: The reference values given in Table 5 ($\gamma_5 = 1.1$) Dotted curve: The reference values given in Table 5, but with $\gamma_5 = 1.11$. (For interpretation of the references to colour in this figure legend, the reader is referred to the web version of this article.)

this is that the stock level is determined by the cost-potential price level ratio ω in this special case of the model. Cf. Section 3.5.1. Since this ratio is not affected by a reduction in the biomass growth (caused by accumulated pollution), the fish biomass equilibrium is unchanged. However, the steady state effort level is decreased because of the reduction in the long run harvest volume. Furthermore, we infer from the fifth row in Table 5 that a partial introduction of the income effect (represented by a finite γ_{11}) increases the fish demand and thereby makes the fishery more profitable which causes a higher level of effort and a lower fish stock biomass in the long run. From the input parameters of the sixth row in Table 5 ("Demand pollution"), we notice that the partial negative effect on the marginal willingness to pay for fish from pollution (represented by finite γ_9 and γ_{10}), makes the fishery less profitable because of reduced demand in the fish market. This implies the existence of an equilibrium state with lower effort and higher biomass.

Table 6
Baseline fishery parameters. The measurement units are $M = Tons$, $C = Euro$, $E = Vessels$ and $T = Year$.

Parameters	Values	Measurement units
K	4000000	M
$A_0 + C_0$	10000	CM^{-1}
q	0.000002	$E^{-1}T^{-1}$
λ/σ	0.000025	ETC^{-1}
c	40000	$CE^{-1}T^{-1}$
γ_6	2	-
γ_{12}	1	-
$\omega = \frac{\gamma_{12}}{\gamma_6}$	$\frac{1}{2}$	-

3.5.3. Impacts of economic growth and pollution on equilibrium and stability in the fishery

Finally, we will illustrate the impacts of the economic growth

Table 5
Summary of numerical cases. Different set of input parameters γ_i, =1, 2, ...,12 and corresponding (u, v)-coordinates in Fig. 7 obtained by means of the procedure (51). The fourth column in Table 5 contains the stable equilibrium values for the nondimensional biomass variable ξ and the nondimensional effort variable η. For the example in Fig. 13 the stable equilibrium values for the nondimensional accumulated pollution variable and the nondimensional production per capita variable are given as $\theta_e = 0.33$ and $\psi_e = 1.2$, respectively. For the example in Fig. 13 the stable equilibrium values for the nondimensional accumulated pollution variable and nondimensional production per capita variable are $\theta_e = 0.13$ and $\psi_e = 1.11$, respectively. For all other examples we have $\theta_e = 0.11$ and $\psi_e = 1.1$.

Numerical examples presented in Section 3.5.

	$(\gamma_1, \gamma_2, ...,\gamma_{12})$	(u, v) (in Fig. 7)	(ξ_e, η_e)
Fig. 8	(0,1,1,1,1.1,2,0.5,0.5,0,0,0,1)	$A = (0, 1.944)$	(0.55,0.46)
Fig. 7	(0,1,1,1,1.1,2,0,0,0,0,0,1)	$B = (0.667, 0)$	(0.5,0.5)
Biomass Growth	(1,1,1,1,1.1,2,0,0,0,0,0,1)	$(0.691, 0)(\approx B)$	(0.5,0.39)
Demand Income	(0,1,1,1,1.1,2,0,0,0,0,0.1,1)	$(0.655, 0)(\approx B)$	(0.45,0.55)
Demand Pollution	(0,1,1,1,1.1,2,0,0,1,0.5,0,1)	$(0.687, 0)(\approx B)$	(0.61,0.39)
Ref. case	(1,1,1,1,1.1,2,0.5,0.5,1,0.5,0.1,1)	$C = (-0.062, 2.352)$	(0.56,0.33)
Fig. 9a	(1,1,1,2,1.1,2,0.5,0.5,1,0.5,0.1,1)	$C = (-0.062, 2.352)$	(0.56,0.33)
Fig. 9b	(1,1,1,1,1.11,2,0.5,0.5,1,0.5,0.1,1)	$(-0.069, 2.420)(\approx C)$	(0.57,0.31)
Fig. 10a	(1,1.1,1,1,1.1,2,0.5,0.5,1,0.5,0.1,1)	$D = (-0.039, 1.968)$	(0.52,0.48)
Fig. 10b	(1,1.1,1,1,1.21,2,0.5,0.5,1,0.5,0.1,1)	$(-0.067, 2.357)(\approx C)$	(0.555,0.335)
Fig. 11	(1,1,1,1,1.1,2,0.5,0.5,1,0.5,0.1,1.72)	$E = (0.271, 1.771)$	(0.89,0)
Fig. 12	(1,1,1,1,1.2,2,0.5,0.5,1,0.5,0.1,1)	$F = (-0.212, 3.352)$	(0.59,0.07)

modelled by means of changes in the parameters r and $\bar{Y}$ in our model. We also consider the influence of the remediation capacity. This situation corresponds to changes in the nondimensional parameters γ_4 and γ_5, and the normalized remediation rate γ_2. In the following numerical analyses all the mechanisms are present, given by means of the parameter values listed in Table 5. We use the following parameter set as the reference case: $\gamma_1 = \gamma_2 = \gamma_3 = \gamma_4 = \gamma_9 = \gamma_{12} = 1$, $\gamma_6 = 2$ $\gamma_5 = 1.1$, $\gamma_7 = \gamma_8 = \gamma_{10} = 0.5$, $\gamma_{11} = 0.1$ and the initial condition as in Fig. 5a and Fig. 8a. The Group 2 input parameters are the same as the ones underlying the computations of the stable fishery equilibrium given in Table 5, and also represented by means of point C in Fig. 7.

Fig. 10a and Fig. 10b show the temporal development of the nondimensional biomass and the nondimensional effort when the short term economic growth and the long term production per capita level are changed. In Fig. 10a we observe that an increase in the short run growth rate will cause increased fishery fluctuations. Both the biomass and the effort are characterized by an increase in the level of oscillations, without actually changing the corresponding equilibrium values. Fig. 10b shows the case where the long term production per capita is increased (measured by means of the nondimensional parameter γ_5). Here the changes in the temporal behaviour of the biomass and the effort are less pronounced. In our example, the equilibrium value of the effort is reduced and the stock size is increased, which follows from a net increase in the cost-price ratio. This means a reduced profitability in the fishery. Fig. 11a and b demonstrate how the remediation rate influences the fishery. Fig. 11a illustrates the impact on the temporal evolution of the biomass and the effort variables, as well as on the equilibrium values, for a partial increase in the remediation rate (by changing $\gamma_2 = 1$ to $\gamma_2 = 1.1$). It is seen that this leads to a reduction in the biomass and an increase in the effort equilibrium values. Moreover, the oscillations become more pronounced as the remediation rate increases. In Fig. 11b we have increased both the remediation rate and the long run production level, but kept the emission-remediation-ratio ι (defined in Table 2) unchanged. In our example we observe minor changes compared to the isolated changes in the remediation rate. Changes in the model parameters may also cause changes affecting the existence of stable equilibrium points for the fishery part of the model. In Fig. 12a we demonstrate how the high relative unit cost of effort makes the fishery unprofitable. This effect is captured within the present nondimensional setting by means of the parameter γ_{12}. By strengthening the general cost effect (which is done by increasing the 'cost' parameter from the reference value $\gamma_{12} = 1$ to $\gamma_{12} = 1.72$), we observe that fishery effort becomes zero, whereas the fish biomass survives and stabilizes at $\xi_e = 1 - \gamma_1\theta_e = 0.89$. This is consistent with the fact that $Q_1 = (0.89, 0, 0.11, 1.1)$ defined by (42) in accordance with (57) is an asymptotically stable equilibrium point in this case. This equilibrium solution with a unprofitable fishery (zero effort), may also follow from combinations of other model mechanism which influences the profitability. For instance it follows that a stronger "Demand pollution" effect (represented by γ_9 and γ_{10}) could also make the fishery unprofitable, i.e and stabilize at Q_1 defined by (42) in accordance with (57). We also notice that the interior stable equilibrium for the reference case ($\gamma_{12} = 1$) is $Q_e = (0.56, 0.33, 0.11, 1.1)$ and that the corresponding boundary equilibrium point Q_1 is unstable in accordance with (57).

In Fig. 13 we demonstrate how the stability acts on the fishery by means of a partial increase in the long run production and income level $\bar{Y}$. Within the present nondimensional setting, this means an increase in the value of the parameter γ_5. In Fig. 6 we have illustrated the identical case for the pollution part of the model. With the selected initial conditions and parameter values, we observe that an increase in the long run production and the income level leads to a relatively rapid decrease in the effort, and eventually to a drop in the stock level. With $\gamma_5 = 1.20$ the fishery becomes less profitable causing low equilibrium effort and a stabilization in biomass density, while in the case with $\gamma_5 = 1.21$ both the fish stock and the fishery activity are wiped out within finite time.

4. Concluding remarks

Since the early 1970s economists and scientists from different fields have been engaged in the research on the consequences of emissions from economic activities on ecosystems. Growing economies often mean higher emissions. In particular, the effect of pollution on marine ecosystems has recently received greater attention from the research community. The ability of the ecosystem to conduct remediation or self-cleaning in order to reduce harmful effects from the pollution appears to be a key issue in this context.

In the present work we have proposed a dynamical model describing the interactions between production and consumption,

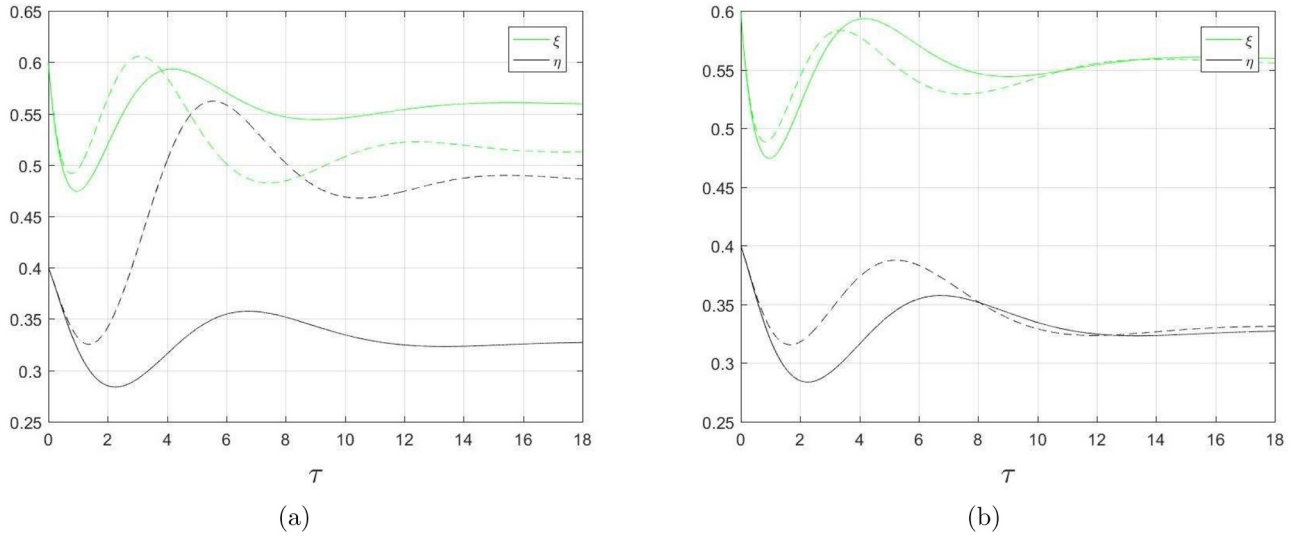

Fig. 11. Impact of remediation and economic growth. Initial condition as in Fig. 5a and Fig. 8b. (a)The impact of increased relative remediation rate (γ_2). The nondimensional biomass ξ (green curve) and the nondimensional effort η (black curve) as function of the nondimensional time τ. Bold curve: The reference values given in Table 5 ($\gamma_2 = 1$). Dotted curve: The reference values given in Table 5, but $\gamma_2 = 1.1$. (b) The nondimensional biomass ξ (green curve) and the nondimensional effort η (black curve) as function of the nondimensional time τ (with higher remediation rate and long run production level, but with an unchanged emission-remediation-ratio.) Bold curve: The reference values given in Table 5 ($\gamma_2 = 1$, $\gamma_5 = 1.1$). Dotted curve: The reference values given in Table 5, but $\gamma_2 = 1.1$ and $\gamma_5 = 1.21$, ($\iota = \gamma_5/\gamma_2 = 1.1$). (For interpretation of the references to colour in this figure legend, the reader is referred to the web version of this article.)

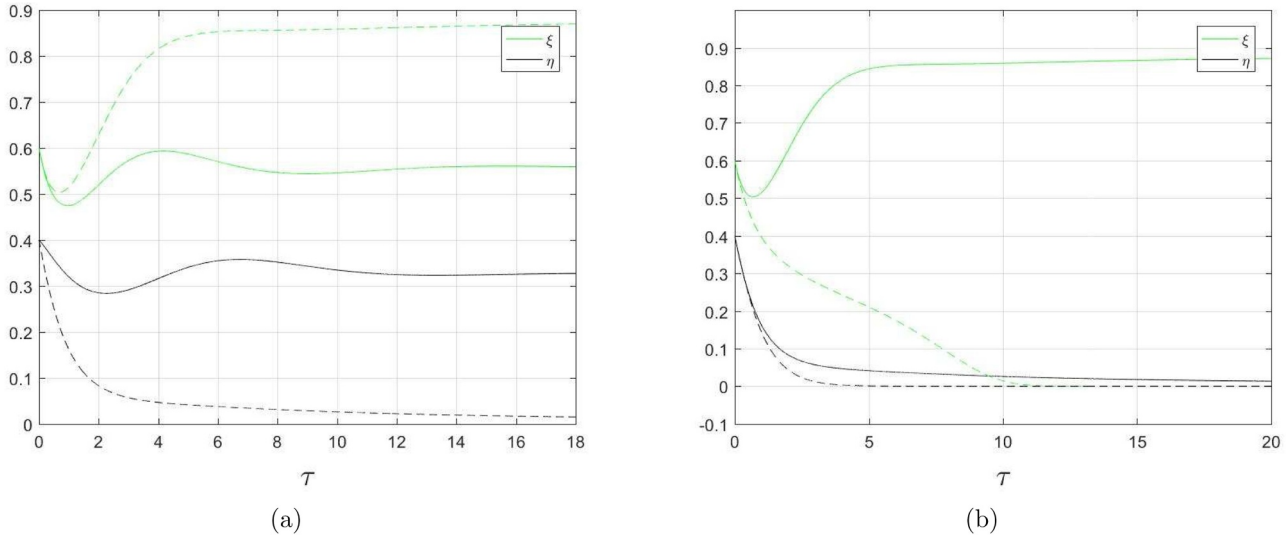

Fig. 12. Examples of a profitable fishery being wiped out. (a) Bold curve: A profitable fishery. The reference values are given in Table 5. Initial condition as in Fig. 5a and Fig. 8b ($\xi_0 = 0.6$, $\eta_0 = 0.4$, $\theta_0 = 0.6$, $\psi_0 = 0.6$). Stable equilibrium: $Q_e = (0.56, 0.33, 0.11, 1.1)$. Dotted curve: The same parameter values as for the bold curve, except $\gamma_{12} = 1.72$ (increased cost level). Initial condition as for the bold curve. $Q_1 = (0.89, 0, 0.11, 1.1)$ given by (42) is a stable equilibrium point. (b) Initial condition, with high level of production per capita (ψ) gives unbounded pollution growth and extinction of the fish stock. Parameter values equal to the reference values given in Table 5, except $\gamma_{12} = 1.72$. Bold curve: (which is the dotted curve in (a)). Initial condition: ($\xi_0 = 0.6$, $\eta_0 = 0.4$, $\theta_0 = 0.6$, $\psi_0 = 0.6$). Dotted curve: Initial condition ($\xi_0 = 0.6$, $\eta_0 = 0.4$, $\theta_0 = 0.6$, $\psi_0 = 1.4$), which is the initial condition marked as point IC_2 in Fig. 4 and also described in Fig. 6.

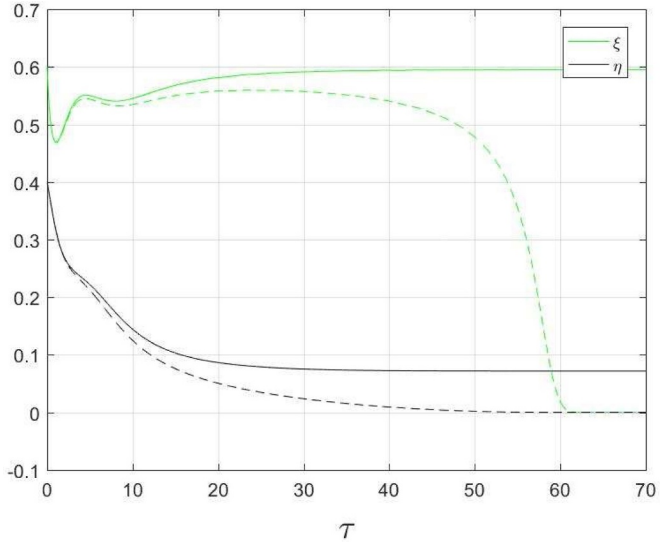

Fig. 13. A profitable fishery wiped out by a high long run production and income level. Development in the nondimensional biomass variable ξ and nondimensional effort variable η is depicted as a function of the nondimensional time τ. Bold curve: $\gamma_5 = 1.20$ and $\gamma_1 = \gamma_9 = 1$, $\gamma_{10} = 0.5$, $\gamma_{11} = 0.1$. Dotted curve: $\gamma_5 = 1.21$ and $\gamma_1 = \gamma_9 = 1$, $\gamma_{10} = 0.5$, $\gamma_{11} = 0.1$. Initial condition as in Fig. 5a and Fig. 8b.

remediation and biomass production. This model decomposes into two parts: In the first part we have formulated a model accounting for the assumption that the production and consumption cause emissions, and that these emissions either remediate or accumulate in the ocean. In the second part, we propose a traditional Gordon-Schaefer fishery model with open access, where the density of damaging emissions can cause a reduction in the biological growth of the fish stock. Additionally, the economic growth is assumed to increase the general income, which may increase the willingness of consumers to buy fish. Finally, in the demand function we also investigate the possibility that pollution may reduce consumers' marginal willingness to pay for the fish, either because the fish quality actually is reduced or at least consumers *believe* that pollution is harming its quality.

As far as we know, the study of remediation or self-cleaning using a dynamical systems theory approach is new in this literature. The key ingredient in the description of this process is the so called *remediation capacity* introduced in Section 2.1. The remediation capacity is a positive and two times continuously differentiable function of the pollution density. This function models the self-cleaning ability of the marine ecosystem. The most prominent feature of the remediation capacity is that it increases for low and moderate levels of the pollutant emission. This means that the marine system is capable of undertaking self-cleaning. However, when the pollution density exceeds a certain threshold, this ability gradually weakens. We have taken care of this property by assuming the remediation capacity to decrease in line with the pollution density in this regime. For large values of the pollution density the remediation capacity will vanish, indicating that the self-cleaning ability of the marine ecosystem is completely destroyed in the case of large emissions of pollutants. It is shown that these assumptions lead to the existence of one stable equilibrium in the economic growth and pollution part of the model. This stable steady state serves as the starting point for the investigation of the consequences that growth and pollution have on the fishery in the long run.

4.1. Main results

First, we notice that when there are only a biomass growth impact from pollution, the harvest volume and the equilibrium effort in the fishery are reduced, while the fish stock equilibrium value remain unchanged. The explanation for this is that the stock level is determined by the cost-potential price level ratio which is constant in this special case of the model. Second, a partial positive income demand effect from the growth, leads to increased profitability, higher equilibrium effort and a lower fish stock. Third, a partial consequence of reduced willingness to pay for fish as pollution increases, gives the opposite conclusion, i.e. a reduced equilibrium effort and a higher fish stock. If this negative effect on the marginal willingness to pay for fish from pollution is strong enough it could make the fishery unprofitable.

Furthermore, we introduce an illustrative example to discuss how growth, emission and remediation may influence the fishery. First we show that an increase in the short term growth in the economy may

affect the effort and stock development over time, but the long term equilibrium is unchanged. However, a partial increase in the long term production per capita, is in our example shown to reduce the equilibrium of fishery effort and increase the stock size, following from a net increase in the cost-price ratio. Moreover, a partial increase in the remediation rate is seen to reduce the biomass equilibrium and increase the long term effort. When both the remediation and the long run growth rate is increased such that the emission-remediation-ratio stays unchanged, the changes in equilibrium effort and biomass values becomes relative small. From the numerical analyses it is seen that economic growth and remediation capacity influences the temporal development in both effort and fish biomass. Finally, we notice that if production per capita exceeds a certain threshold (causing high emissions of pollutants) the fishery activity become less profitable, and within finite time the effort go to zero and the fish stock become extinct.

The outcome of the stability analysis shows that it is possible to have bistability in the present modelling framework. This means that there are parameter regimes which produce coexistence of a stable boundary equilibrium point (Q_1) and a stable interior equilibrium point (Q_e) in the first orthant of the phase space. This property will lead to a division of the first orthant of the phase space into a union of disjoint attractor basins for the two equilibrium points. However, for the concrete examples we have explored numerically in the present paper we do not observe the bistability phenomenon.

4.2. Possible extensions

We emphasize that our reasoning is based on a simplified and conceptual model where we have made many simplifying assumptions. For instance, we only consider one typical exploited wild fish stock and the consequences of economic growth and pollution on the growth potential of that fish stock and the market where fish products are sold. In reality, economic activities and pollution can have multiple external and economic effects on oceans and coastal areas, and thereby exert more complex dynamical influences on the fisheries.

For simplicity we have assumed that the biological growth satisfies the conditions of the Verhulsts population growth model, and used the Gordon-Schaefer harvest production function. Modifications of these assumptions, as discussed in e.g. Clark (2010), Flaaten (2018) or Eide (2018), represent possible extensions of the present analysis.

Another interesting extension of the model would be to describe in much greater detail how various pollution types could affect the fish stocks, and to analyze dynamical effects stemming from these different emission sources. For instance, some activities may cause marine emissions that harm the fishery at different stages. Following Cushing (2013) and the references therein, one could incorporate these effects by including absolute and distributed time lag effects in the modelling framework. We expect that this will change the dynamical features as compared with the output from the present model.

Additionally, an aspect that would be interesting to consider is how the economic growth and the ocean pollution affect ecological systems where the fish stock is only one important element. Widening the biological focus could reveal different effects on various species that are interrelated in the ecological system, and such an analysis could capture important dynamical aspects of pollution on the fisheries.

Another possible extension consists of adding time dependent stochastic effects. This is indeed motivated by the fact that quantities in both model blocks are subject to uncertainties, and should thus be modelled as stochastic processes. This will eventually lead to a modeling framework which should be dealt within the theory of stochastic dynamical systems. Here we could follow the line of thought in for example Evans (2012) and Øksendal (2003), i.e. that we rewrite the model as an autonomous dynamical system of first order equations and thereafter incorporate the stochastic effects as additive noise terms in this system. We list this problem as a topic for future research.

Moreover, the consequences of economic growth and pollution on harvesting and fish markets may be more complex and sophisticated than captured by our model. For instance, we have made an oversimplification by assuming a proportional relationship between the economic growth and the pollution density. Following the line of thought as in Perman et al. (2003), a more realistic relationship might be that the emissions - due to technological progress and steadily more environmental awareness in production and consumption - can be modelled by means of a concave function of the production per capita. We have also ignored that fishery activities could be a source of both economic growth and ocean pollution. If so, we would then have a feedback mechanism from the fishery on the economic growth and pollution level that we have disregarded in our approach.

Our analysis presumes that the fishery is characterized by an open access regime. In future investigations one should also focus on environmental and fishery policies. Such policies could be based on maximizing social welfare in a dynamic perspective, i.e. identifying preferred allocations of possible stable equilibrium states of economic growth, emissions, size of the fish stock and the effort in harvesting. Here public regulatory mechanisms can play a role. Such mechanisms could work to limit the economic growth, reduce the emissions impact of growth or find ways of increasing the remediation capacity. Regulations might take the form of renovation policies, or use indirect means, such as taxes and subsidies to bring about a preferable development.

Developing the model further by taking into account one or more of the possibly complicating aspects mentioned above, is an interesting task for future research on marine pollution and fishery dynamics.

Acknowledgements

The present work was initiated in Spring 2018 when J. Wyller was Guest Professor at the Department of Applied Mathematics and Computer Science, Technical University of Denmark (DTU) and completed in Autumn 2018 when J. Wyller was Guest Professor at Department of Mathematics, Natural Sciences and Information Technologies, Derzhavin Tambov State University, Russia. J. Wyller will like to express his sincere gratitude to both DTU and Derzhavin Tambov State University for their kind hospitality during his stays. The authors are grateful to Professor Arcady Ponosov and Professor Bjørn Fredrik Nielsen (Norwegian University of Life Sciences), Professor Mads Peter Sørensen and Associate Professor Uffe Høgsbro Thygesen (Technical University of Denmark) and Professor Ola Flåten and Professor Arne Eide (The Arctic University of Norway) for fruitful and stimulating discussions during the preparation phase of this paper. The authors would also like to thank the reviewers for constructive remarks. This research work was supported by the Norwegian University of Life Sciences and The Research Council of Norway, project number 239070.

Appendix A. The scaling properties of the economic growth function and the remediation capacity.

Let Φ be a realvalued function which depends on the parameters $a_1, a_2, \cdots, a_N$. We assume that there is a function $\tilde{\Phi}$ so that the scaling property

$$\Phi[x; \mathbf{a}] = C_\Phi \tilde{\Phi}[z; \Pi] \tag{A.1}$$

is fulfilled. Here $\mathbf{a} = (a_1, a_2, \cdots, a_N) \in \mathbb{R}^N$ is a parameter vector. The variable z is defined as $z = x/A_\Phi$ where $[A_\Phi] = [x]$. A_Φ and C_Φ are monomials in the components $a_1, a_2, \cdots, a_N$. Moreover, $[\Phi] = [C_\Phi]$. The components $\Pi_1, \cdots, \Pi_m$ of the vector $\Pi \in \mathbb{R}^{\mathbf{m}}$ are independent, dimensionless monomials of the components $a_1, a_2, \cdots, a_N$ of the parameter vector $\mathbf{a}$. According to Buckinghams Π-theorem, $m = N - r$ where r is the rank of the dimension

matrix deduced from the parameters $a_1, a_2, \cdots, a_N$ (Logan, 1987).

This means that $\tilde{\Phi}$ is a dimensionless function of the dimensionless variable z and the dimensionless parameters $\Pi_1, \cdots, \Pi_{N-r}$. Notice that the scaling property (A.1) ensures that all the terms in Φ have the same dimension.

Let $\mathbf{a}$ be a parameter vector which contains the parameters in our model and that the vector Π contains the independent, nondimensional parameters constructed by means of $\mathbf{a}$. We assume that the remediation capacity g described in Section 2 satisfies a scaling property of the type (A.1) i.e.

$$\theta = \frac{S}{A_g}, \quad g\left[S; \mathbf{a}\right] = C_g \tilde{g}\left[\theta, \Pi\right] \tag{A.2}$$

This yields the nondimensional version

$$\theta' = \frac{\varrho B_g}{\sigma A_g}\psi - \frac{\rho C_g}{\sigma A_g}\tilde{g}\left[\theta; \Pi_1, \Pi_2, \Pi_3, \cdots, \Pi_N\right]$$

of the pollution Eq. (7). Here B_g is the amplitude factor of the general production and income function Y i.e. $Y = B_g\psi$. Moreover, we have made use of $\tau = \sigma t$. We choose

$$C_g = A_g = a, \quad B_g = \frac{\sigma a}{\varrho} \tag{A.3}$$

and end up with the nondimensional version

$$\theta' = \psi - \gamma_2 \tilde{g}\left[\theta; \Pi_1, \Pi_2, \Pi_3, \cdots, \Pi_{N-r}\right]$$

of the pollution equation. Here $\gamma_2 = \rho/\sigma$ and $a_1 \equiv a$.[5]

We finally assume that the economic growth function f obeys a scaling property of the type (A.1) i.e.

$$\psi = \frac{Y}{A_f}, \quad f\left[Y; \mathbf{a}\right] = C_f \tilde{f}\left[\psi, \Pi\right] \tag{A.4}$$

By using $Y = A_f\psi$ and $\tau = \sigma t$ we derive

$$\psi' = \frac{rC_f}{\sigma A_f}\tilde{f}\left[\psi; \Pi_1, \Pi_2, \Pi_3, \cdots, \Pi_{N-r}\right] \tag{A.5}$$

from (1). In this case we choose

$$C_f = A_f = \frac{\sigma a}{\varrho}, \quad \Pi_1 = \frac{\bar{Y}}{A_f} = \frac{\varrho \bar{Y}}{\sigma a} \tag{A.6}$$

and end up with

$$\psi' = \gamma_4 \tilde{f}\left[\psi; \gamma_5, \Pi_2, \Pi_3, \cdots, \Pi_N\right] \tag{A.7}$$

Here $\gamma_4 = \frac{r}{\sigma}$ and $\gamma_5 = \frac{\varrho \bar{Y}}{\sigma a}$.

Appendix B. Invariant regions.

We first prove the following lemma:

Lemma 1. *Assume that* $\gamma_5 \geq \gamma_2 R(0; \gamma_3)$. *Then the set* Σ_2 *defined by*

$$\Sigma_2 = \{(\theta, \psi) \in \mathbb{R}^2; \theta > 0, \psi > \gamma_2 R(0; \gamma_3)\} \tag{B.1}$$

is an invariant region of the subsystem (32) i.e.

$$\Psi^\tau(\Sigma_2) \subseteq \Sigma_2$$

Here $\Psi^\tau: \mathbb{R}^2 \to \mathbb{R}^2$ *is the flow induced by the system (32).*

Proof. The smooth vectorfield $\mathbf{F}_2: \mathbb{R}^2 \to \mathbb{R}^2$ defining the dynamical system (32) is given by

$$\mathbf{F}_2(\theta, \psi) = \begin{pmatrix} \psi - \gamma_2 R(\theta; \gamma_3) \\ \gamma_4 \tilde{f}(\psi; \gamma_5) \end{pmatrix}$$

Assume that (θ, ψ) belongs to the first quadrant of the θ, ψ-plane i.e. $\theta, \psi \geq 0$. We readily find flux conditions

$$\mathbf{F}_2(0, \psi)\cdot\mathbf{e}_\theta = \psi - \gamma_2 R(0; \gamma_3)$$

$$\mathbf{F}_2(\theta, 0)\cdot\mathbf{e}_\psi = \gamma_4 f(0; \gamma_5)$$

on the boundaries of the first quadrant. Here $\mathbf{e}_\theta$ and $\mathbf{e}_\psi$ are the unit vectors along the θ- and ψ-axis, respectively. By assumption, $f(0; \gamma_5) > 0$. Hence $\mathbf{F}_2(\theta, 0)\cdot\mathbf{e}_\psi > 0$ from which it follows that the orbits of (32) are directed inwards into the first quadrant at points located on the positive θ-axis. Next,

[5] Here and in the sequel we make us of the definitions and the notations introduced in (17).

we observe that $\mathbf{F}_2(0, \psi)\cdot\mathbf{e}_\theta > 0$ if $\psi > \gamma_2 R(0; \gamma_3)$. This means that no orbit can leave the first quadrant across the part of the ψ-axis for which $\psi \geq \gamma_2 R(0; \gamma_3)$. In the complementary regime, $0 \leq \psi < \gamma_2 R(0; \gamma_3)$, the directed orbits leave the first quadrant.

Let us examine the region Σ_2 defined by (B.1).

Assume first that $0 < \gamma_5 < R(0; \gamma_3)$. In this case $\psi' < 0$, $\theta' < 0$ for points located on the horizontal line segment $\psi = \gamma_2 R(0; \gamma_3)$, $0 < \theta < \theta_e$ where $\theta = 0$ and $\theta = \theta_e > 0$ are the two solutions of the equation $R(\theta; \gamma_3) = Re(0; \gamma_3)$. This means that there are orbits starting in Σ_2 leaving this region. Hence Σ_2 is not an invariant region in this case. Notice the fate of the orbits when they have left Σ_2: The ψ-coordinate of these orbits will approach $\psi = \gamma_5$ whereas the θ-coordinate will decrease with time. In accordance with the flux condition $\mathbf{F}_2(0, \psi)\cdot\mathbf{e}_\theta < 0$ on the line segment $0 < \psi < \gamma_2 R(0; \gamma_3)$, $\theta = 0$ these orbits will then leave the first quadrant through this line segment within finite time.

Next, let us investigate the regimes when $\gamma_5 \geq \gamma_2 R(0; \gamma_3)$. In this case $\psi' > 0$ on the horizontal line $\psi = \gamma_2 R(0; \gamma_3)$, $\theta > 0$ from which it follows that all the orbits starting on this line will enter Σ_2. In the case $\gamma_2 R(0; \gamma_3) \leq \gamma_5 \leq \gamma_2 R(\theta_{\max}; \gamma_3)$, the equilibrium point (θ_-, γ_5) acts as an attractor for a subset of Σ_2 whereas the remaining part of Σ_2 evolves into a state for which $\psi \to \gamma_5$, $\theta \to \infty$. For $\gamma_5 > \gamma_2 R(\theta_{\max}; \gamma_3)$ all the points in Σ_2 are moved into the state $\psi \to \gamma_5$, $\theta \to \infty$. □

We easily prove the following lemma which holds true for any dynamical system of the Lotka-Volterra type:

Lemma 2. *Let F and G be given by (19) and (20). The initial value problem*

$$\begin{aligned} \xi' &= \xi F(\xi, \eta, \theta, \psi), \quad \xi(0) = \xi_0 \\ \eta' &= \eta G(\xi, \eta, \theta, \psi), \quad \eta(0) = \eta_0 \end{aligned} \tag{B.2}$$

is equivalent with the fixed point problem

$$\begin{aligned} \xi(\tau) &= \xi_0 \exp\left[\int_0^\tau F(\xi(s), \eta(s), \theta(s), \psi(s))ds\right] \\ \eta(\tau) &= \eta_0 \exp\left[\int_0^\tau G(\xi(s), \eta(s), \theta(s), \psi(s))ds\right] \end{aligned} \tag{B.3}$$

Proof. Assume that (B.3) is satisfied. For $\tau = 0$ we have $\xi(0) = \xi_0$ and $\eta(0) = \eta_0$. Differentiation of the expression (B.3) with respect to τ shows that ξ and η satisfy the differential equations in (B.3). Next, assume that (B.3) is satisfied. The fact that $(\ln(|\xi|))' = \xi'/\xi = F$ and $(\ln(|\eta|))' = \eta'/\eta = G$, a subsequent integration and the initial condition $\xi(0) = \xi_0$, $\eta(0) = \eta_0$, implies the fixed point problem (B.3). □

Lemma 2shows that $(\xi_0, \eta_0 = (0, 0)$ if and only if $(\xi(\tau), \eta(\tau)) = (0, 0)$ for $\tau \in I_0$, where I_0 is the existence interval for the solution. Moreover, we have $\xi_0 > 0$ ($\eta_0 > 0$) if and only if $\xi(\tau) > 0$ ($\eta(\tau) > 0$) for $\tau \in I_0$.

Hence, by appealing to Lemma 1 and Lemma 2, we end up with the following result:

Theorem 1. *Assume that $\gamma_5 \geq \gamma_2 R(0; \gamma_3)$. Then the set Σ defined by (31) is an invariant region of the dynamical system (30) i.e.*

$$\Phi^\tau(\Sigma) \subseteq \Sigma$$

Here $\Phi^\tau: \mathbb{R}^4 \to \mathbb{R}^4$ is the flow of the dynamical system (30). Moreover, the sets Σ_1 and Σ_2 defined in Section 3.2.2 and Section 3.2.3, respectively, are invariant sets of the dynamical system (30) i.e.

$$\Phi^\tau(\Sigma_i) \subseteq \Sigma_i, \quad i = 1, 2$$

Appendix C. Existence of equilibrium points in the interior of the first orthant of the phase space.

Here we investigate the properties of the polynomial Q_3 defined by (47). We start out by determining the signs of the coefficients α_i, $i = 0, 1, 2, 3$ in the polynomial $\mathcal{P}_3$ defined by (46). We first notice that the positivity of γ_8 and γ_{12} implies that $\alpha_0 < 0$. Moreover, since $\frac{\theta_e}{\theta_e + \gamma_{10}} < 1$, we find that

$$\alpha_3 < \gamma_7 - \gamma_6 + \gamma_9 - \gamma_5\gamma_{11}$$

Then, by the constraints in (13) and the definition (17) we find that

$$\gamma_7 + \gamma_9 - \gamma_6 < 0$$

from which it follows that $\alpha_3 < 0$. By observing that

$$\alpha_2 = -\alpha_3(1 - \gamma_1\theta_e) + \gamma_{12}$$

we immediately conclude that $\alpha_2 > 0$. The parameter α_1 is sign-indefinite. The signs of α_0, α_1, α_2, α_3 imply that the coefficients μ and γ of the polynomial Q_3 are strictly positive whereas ν is sign indefinite. Now, since $Q_3(\xi_e; \mu, \nu, \gamma) \to -\infty$ as $\xi_e \to -\infty$ and $Q_3(0; \mu, \nu, \gamma) > 0$, we conclude that Q_3 has at least one negative zero. This means that Q_3 has maximum two positive zeros. In order to extract more information, we study the monotonicity property of Q_3. Simple calculation shows that

$$Q_3'(\xi_e; \mu, \nu, \gamma) = 3((\xi_e - \mu)^2 + \nu - \mu^2)$$

For $\nu \geq \mu^2$, Q_3 is increasing and hence we have no positive zeros in this case. In the complementary regime $\nu < \mu^2$ we get two extreme points $\xi_\pm$ given as

$$\xi_\pm = \mu \pm \sqrt{\mu^2 - \nu}$$

Further analysis shows that $\xi_- \leq 0 < \xi_+$ if $\nu \leq 0$, whereas $0 < \xi_- < \xi_+$ for $0 < \nu < \mu^2$. We notice that $Q_3(\xi_-; \mu, \nu, \gamma) > 0$ in both cases. For the extreme

point ξ_+ the corresponding function value $Q_3(\xi_+; \mu, \nu, \gamma)$ may change sign. If $Q_3(\xi_+; \mu, \nu, \gamma) < 0$, we will get two positive real zeros. If we take into account the restriction $0 < \xi_e < 1 - \gamma_1\theta_e$, we find that if $Q_3(\alpha_e; 1, u, v) < 0$ (with $\alpha_e \equiv \mu^{-1}(1 - \gamma_1\theta_e)$ and $u = \nu/\mu^2$, $v = \gamma/\mu^3$), we have only one positive zero in the interval $(0, 1 - \gamma_1\theta_e)$ whereas if $Q_3(\alpha_e; 1, u, v) > 0$ both positive zeros are located in this interval. The results of this investigation are summarized in Table 4.

References

Arnold, V.I., 1988. Geometrical Methods in the Theory of Ordinary Differential Equations. Springer Verlag, Boston, USA.

Bråte, I.L.N., Eidsvoll, D.P., Steindal, C.C., Thomas, K.V., 2016. Plastic ingestion by atlantic cod (gadus morhua) from the norwegian coast. Mar. Pollut. Bull. 112 (1–2), 105–110.

Chakraborty, K., Jana, S., Kar, T., 2012. Effort dynamics of a delay-induced prey–predator system with reserve. Nonlinear Dyn. 70 (3), 1805–1829.

Chen, X., Alfnes, F., Rickertsen, K., 2015. Consumer preferences, ecolabels, and effects of negative environmental information. AgBioForum 18 (3), 327–336.

Clark, C., 2010. Mathematical Bioeconomics. the Mathematics of Conservation. New York, NY (USA); John Wiley and Sons Inc.

Copes, P., 1970. The backward-bending supply curve of the fishing industry. Scott. J. Polit. Econ. 17 (1), 69–77.

Cushing, J.M., 2013. Integrodifferential Equations and Delay Models in Population Dynamics. 20 Springer Science & Business Media, Berlin, Heidelberg, New York.

Drossel, B., McKane, A.J., Quince, C., 2004. The impact of nonlinear functional responses on the long-term evolution of food web structure. J. Theor. Biol. 229 (4), 539–548.

dArge, R.C., 1971. Essay on economic growth and environmental quality. Swedish J. Econ. 73 (1), 25–41.

Eide, A., 2018. Introduction to fisheries economics by the use of wolfram language and mathematica. Arne Eide.

Evans, L.C., 2012. An Introduction to Stochastic Differential Equations. 82 American Mathematical Soc., Berkley.

Flaaten, O., 2018. Fisheries Economics and Management, 2nd. Ola Flaaten and bookboon.com.

Flaaten, O., Schulz, C.E., 2010. Triple win for trade in renewable resource goods by use of export taxes. Ecol. Econ. 69 (5), 1076–1082.

Foley, N.S., Armstrong, C.W., Kahui, V., Mikkelsen, E., Reithe, S., 2012. A review of bioeconomic modelling of habitat-fisheries interactions. Int. J. Ecol. 2012, 1–11.

Fonner, R., Sylvia, G., 2014. Willingness to pay for multiple seafood labels in a niche market. Mar. Resour. Econ. 30 (1), 51–70.

Førsund, F., Strøm, S., 1980. Environmental and resource economics. (Miljø og ressursøkonomi). Universitetsforlaget, Oslo, Norway. (In Norwegian)

Garzon, C.A., Rey, M.C., Sarmiento, P.J., Cardenas, J.C., 2016. Fisheries, fish pollution and biodiversity: choice experiments with fishermen, traders and consumers. Econ. Polit. 33 (3), 333–353.

Ghosh, B., Kar, T., 2014. Sustainable use of prey species in a prey–predator system: jointly determined ecological thresholds and economic trade-offs. Ecol. Modell. 272, 49–58.

Gibb, R., Bunce, M., Mee, L.D., Rodwell, L.D., Rewhorn, S., 2017. Sources, fate and effects of microplastics in the marine environment: a global assessment. Glob. Chang Biol. 9, 10.

Guckenheimer, J., Holmes, P., 1983. Nonlinear Oscillations, Dynamical Systems, and Bifurcations of Vector Fields. Springer-Verlag, New York, USA.

Haavelmo, T., 1971. The pollution problem from social science point of view (forurensingsproblemet fra samfunnsvitenskapelig synspunkt). Sosialøkonomen (4), 5–8. (In Norwegian)

Hallanger, I.G., Gabrielsen, G.W., 2018. Plastic in the European Arctic. Technical Report. Norwegian Polar Insitute.

Hoagland, P., Jin, D., Kite-Powell, H., 2003. The optimal allocation of ocean space: aquaculture and wild-harvest fisheries. Mar. Resour. Econ. 18 (2), 129–147.

Hofbauer, J., Sigmund, K., 1998. Evolutionary Games and Population Dynamics. Cambridge university press, Cambridge, USA.

Islam, M.S., Tanaka, M., 2004. Impacts of pollution on coastal and marine ecosystems including coastal and marine fisheries and approach for management: a review and synthesis. Mar. Pollut. Bull. 48 (7), 624–649.

Keeler, E., Spence, M., Zeckhauser, R., 1971. The optimal control of pollution. J Econ Theory 4, 19–34.

Logan, J.D., 1987. Applied Mathematics: A Contemporary Approach, New York: J. New York, NY (USA); John Wiley and Sons Inc.

Martinez, N.D., Williams, R.J., Dunne, J.A., 2006. Diversity, complexity, and persistence in large model ecosystems. In: Pascual, M., Dunne, J. (Eds.), Ecological networks: linking structure to dynamics in food webs, pp. 163–185.

Mikkelsen, E., 2007. Aquaculture-fisheries interactions. Mar. Resour. Econ. 22 (3), 287–303.

Øksendal, B., 2003. Stochastic Differential Equations. Springer-Verlag Berlin Heidelberg. Springer-Verlag, Berlin Heidelberg.

Paul, P., Kar, T., Ghorai, A., 2016. Ecotourism and fishing in a common ground of two interacting species. Ecol. Modell. 328, 1–13.

Perman, R., Ma, Y., McGilvray, J., Common, M., 2003. Natural Resource and Environmental Economics. Pearson, Essex, England.

Perrings, C., 2016. The economics of the marine environment: a review. Environ. Econ. Policy Stud. 18 (3), 277–301.

Regnier, E., Schubert, K., 2016. To what extent is aquaculture socially beneficial? Atheoretical analysis. Am. J. Agric. Econ. 99 (1), 186–206.

Smith, H., 1995. Monotone Dynamical Systems: An Introduction to Competitive and Cooperative Systems, ams Math. Surveys and Monographs, vol. 41. American Mathematical Society, Providence RI.

Smith, V.L., 1969. On models of commercial fishing. J.Polit.Econ. 77 (2), 181–198.

Solow, R.M., 1956. A contribution to the theory of economic growth. Q. J. Econ. 70 (1), 65–94.

Strøm, S., 1971. A simplified analysis of a pollution problem. (en forenklet analyse av et forurensingsproblem). Sosialøkonomen (10), 23–34. (In Norwegian)

Strøm, S., 1972. Dynamics of Pollution and Waste Treatment Activities. University of Oslo, Oslo, Norway.

Tietenberg, T., Lewis, L., 2014. Environmental and Natural Resource Economics. Pearson, Essex, England.

Watson, S.C., Paterson, D.M., Queirós, A.M., Rees, A.P., Stephens, N., Widdicombe, S., Beaumont, N.J., 2016. A conceptual framework for assessing the ecosystem service of waste remediation: in the marine environment. Ecosyst. Serv. 20, 69–81.

Wessells, C.R., Anderson, J.G., 1995. Consumer willingness to pay for seafood safety assurances. Journal of Consumer Affairs 29 (1), 85–107.

Whitehead, J.C., 2006. Improving willingness to pay estimates for quality improvements through joint estimation with quality perceptions. Southern Economic Journal 73 (1), 100–111.

Williams, C., 1996. Combatting marine pollution from land-based activities: Australian initiatives. Ocean & coastal management 33 (1), 87–112.